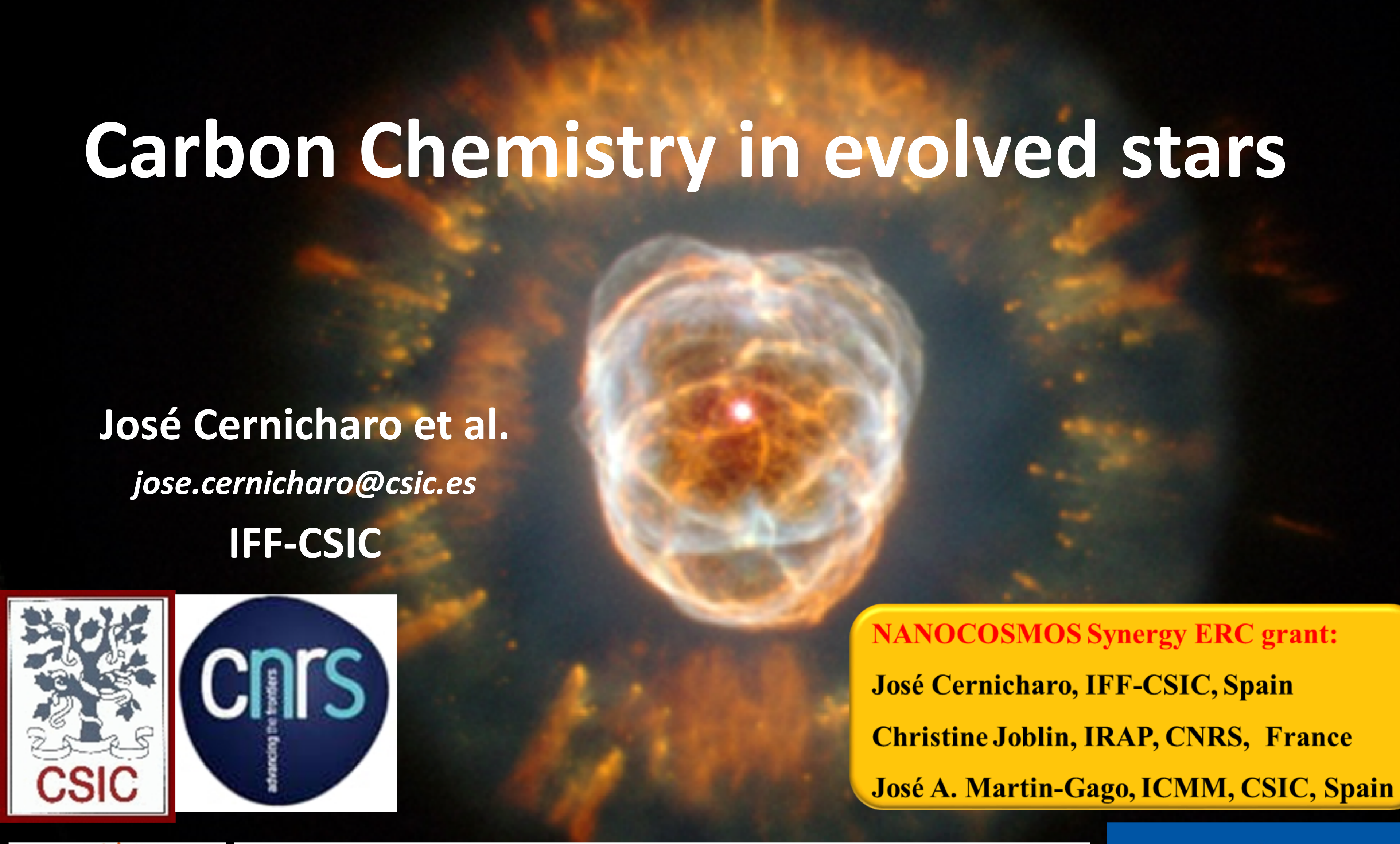

# Carbon Chemistry in evolved stars

**José Cernicharo et al.**
*jose.cernicharo@csic.es*
IFF-CSIC

**NANOCOSMOS Synergy ERC grant:**

José Cernicharo, IFF-CSIC, Spain
Christine Joblin, IRAP, CNRS, France
José A. Martin-Gago, ICMM, CSIC, Spain

European Research Council
Established by the European Commission

# Red giant AGB star

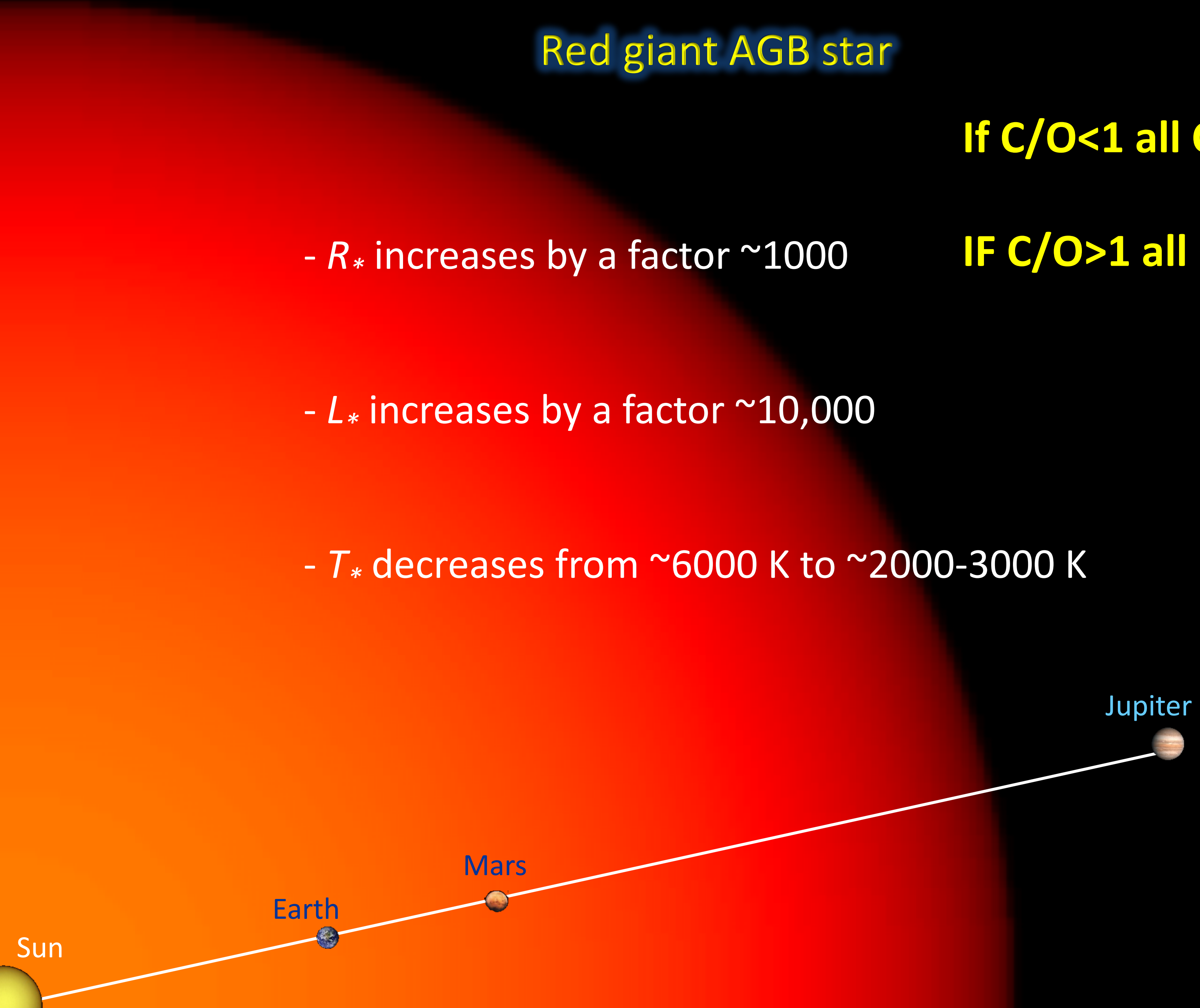

**If C/O<1 all C in CO**

**IF C/O>1 all O in CO**

- $R_*$ increases by a factor ~1000

- $L_*$ increases by a factor ~10,000

- $T_*$ decreases from ~6000 K to ~2000-3000 K

# IRC+10216

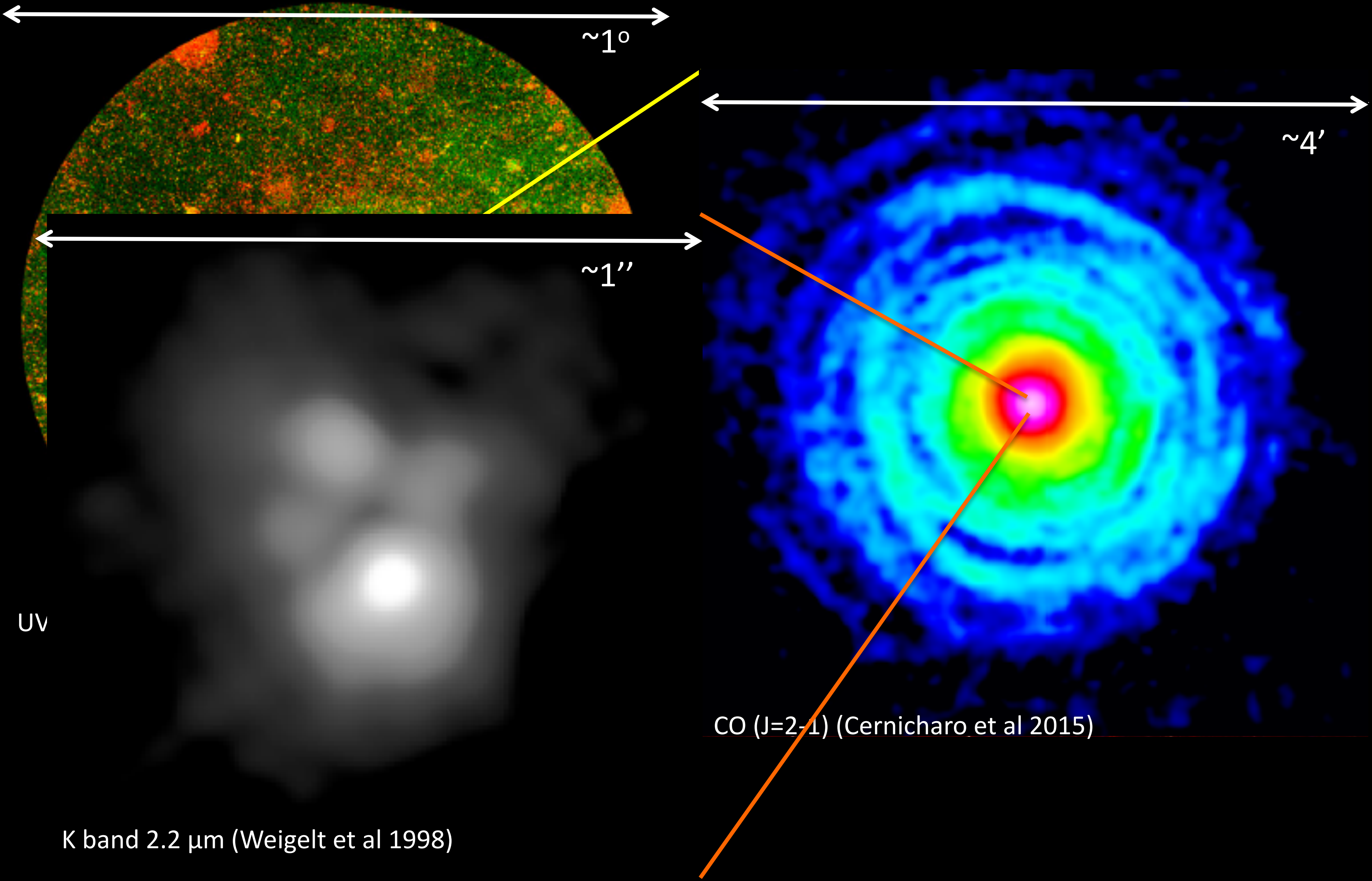

CO (J=2-1) (Cernicharo et al 2015)

K band 2.2 µm (Weigelt et al 1998)

# Circumstellar envelopes around AGB stars

AGB stars lose mass through an isotropic wind

producing an extended circumstellar envelope of gas and dust

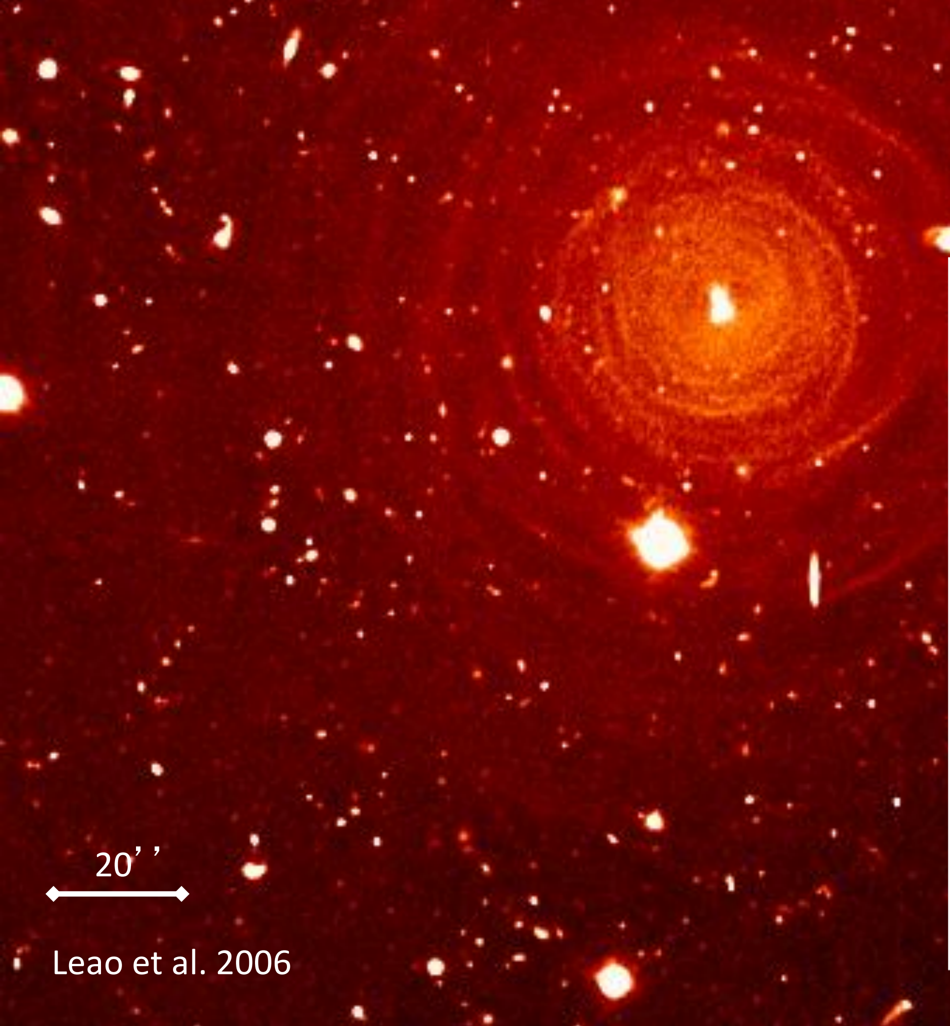

Leao et al. 2006

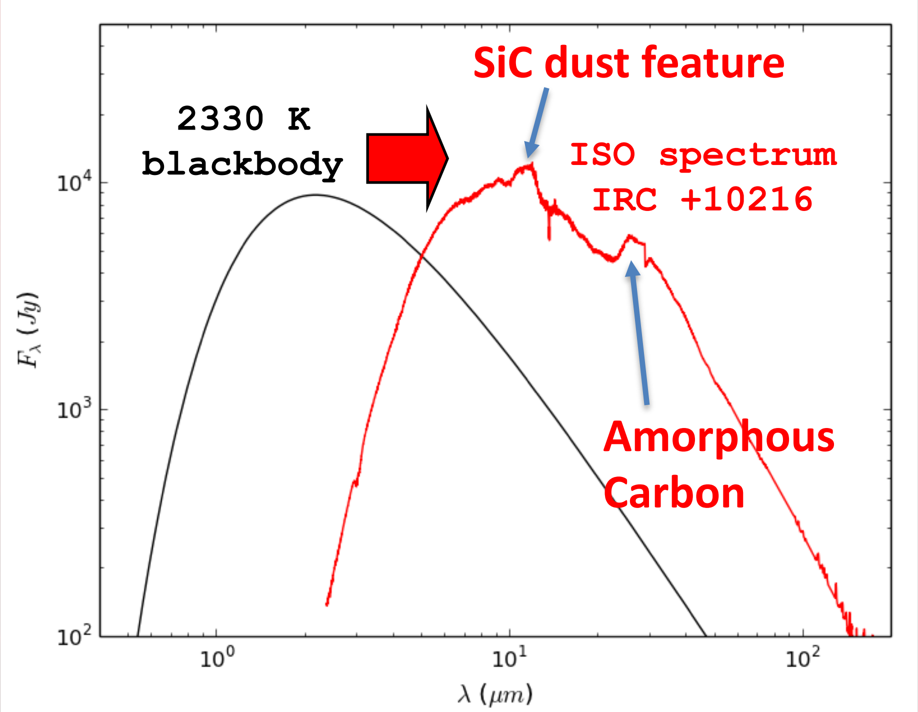

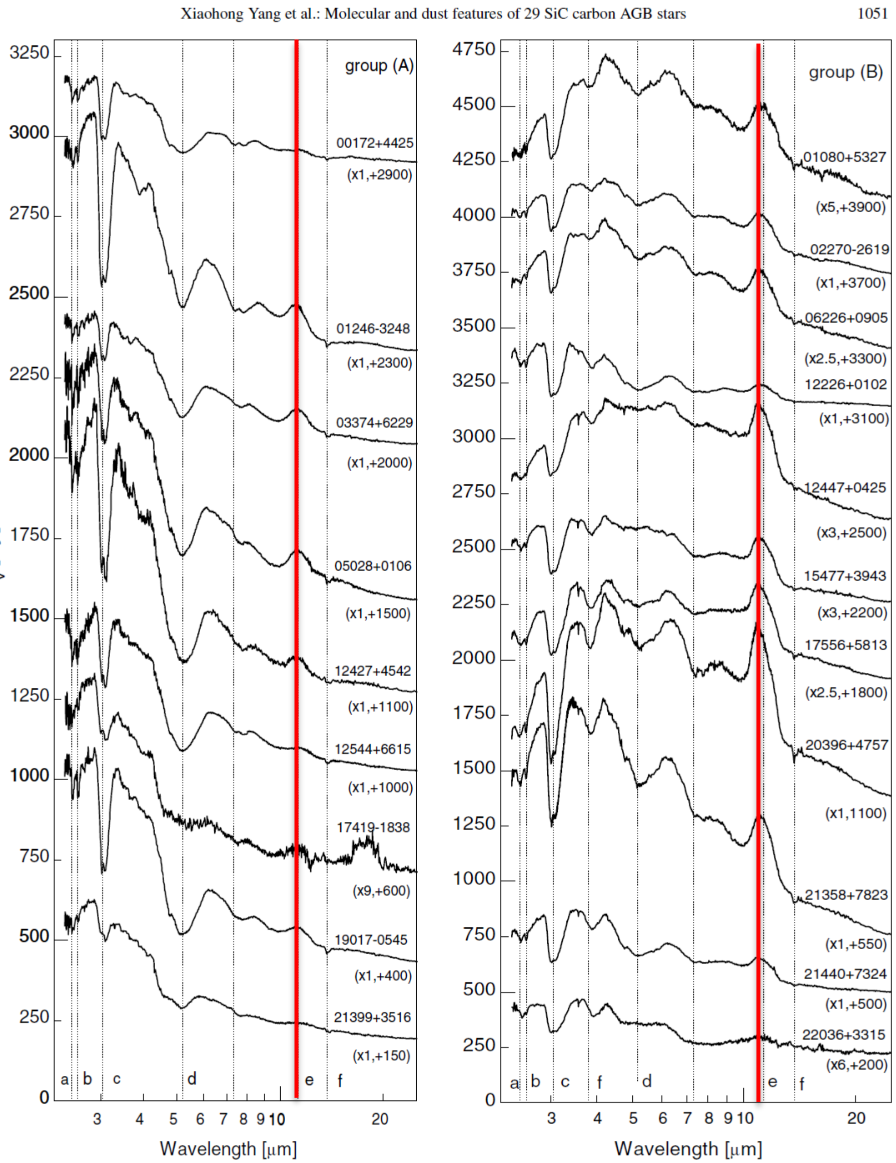

Xiaohong Yang et al.: Molecular and dust features of 29 SiC carbon AGB stars 1051

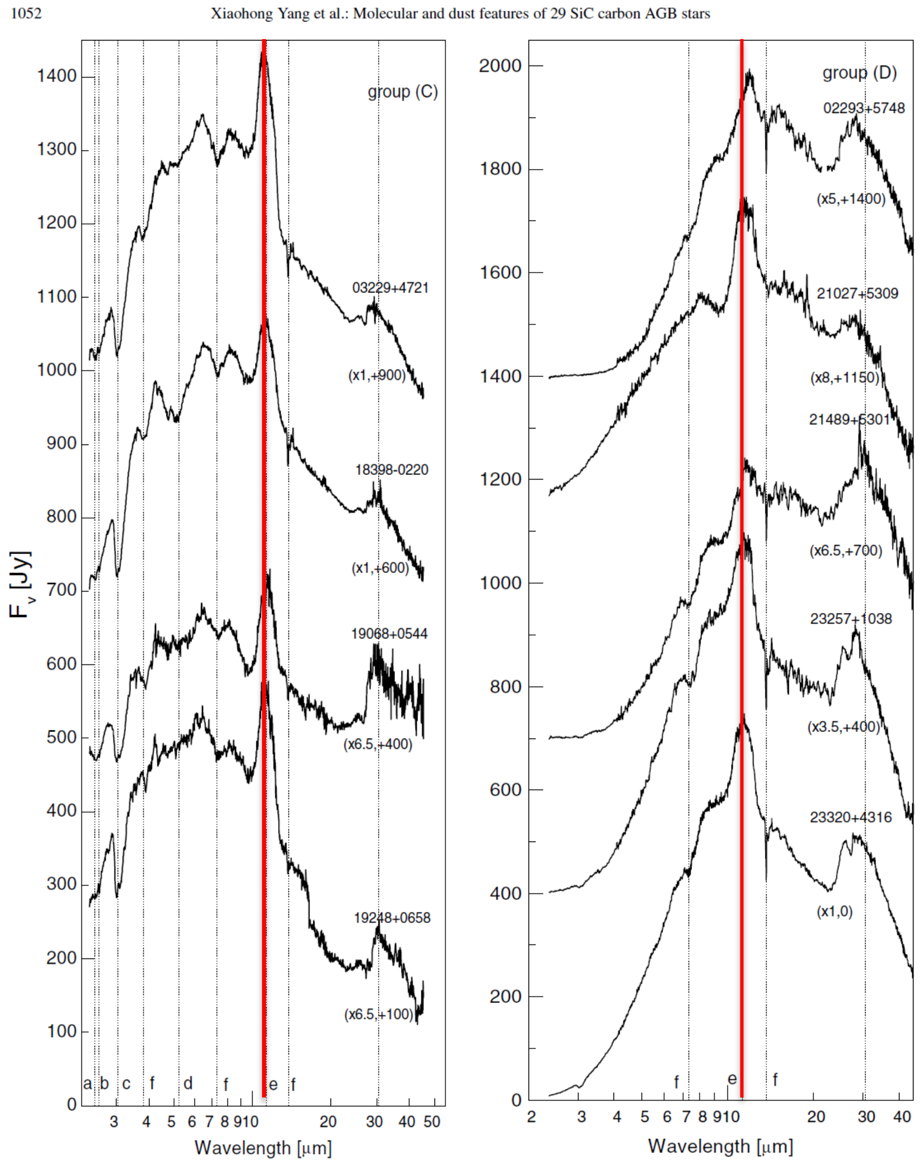

1052 Xiaohong Yang et al.: Molecular and dust features of 29 SiC carbon AGB stars

Yang et al., 2004, A&A, 414, 1049; see also Yamamura et al., 1997, Ap&SS, 255,351
See Chan and Kowk 1990, A&A, 237, 354, for an analysis of the LRS-IRAS spectrum of carbon stars. β–SiC found in presolar meteorites !!!

The Astrophysical Journal, 840:117 (15pp), 2017 May 10

# Nucleation of Small Silicon Carbide Dust Clusters in AGB Stars

David Gobrecht[1,4], Sergio Cristallo[1], Luciano Piersanti[1], and Stefan T. Bromley[2,3]

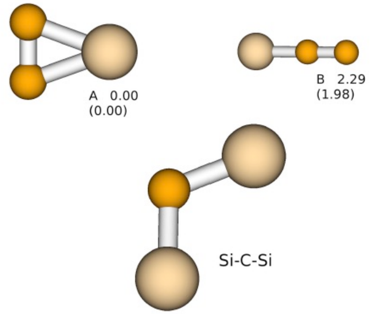

**Figure 1.** The two stable $SiC_2$ clusters and the $Si_2C$ ground state with relative energies (in eV).

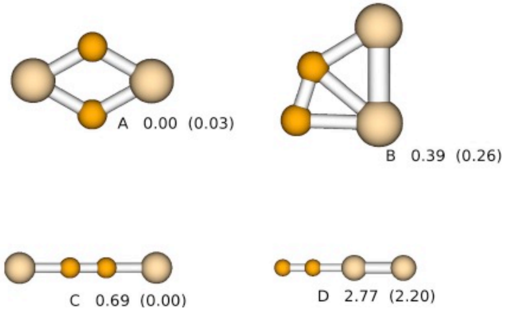

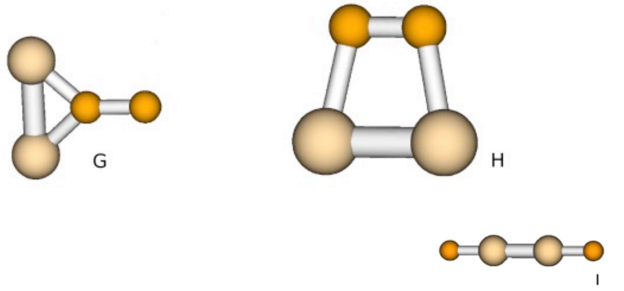

**Figure 3.** Transition states of $Si_2C_2$ clusters.

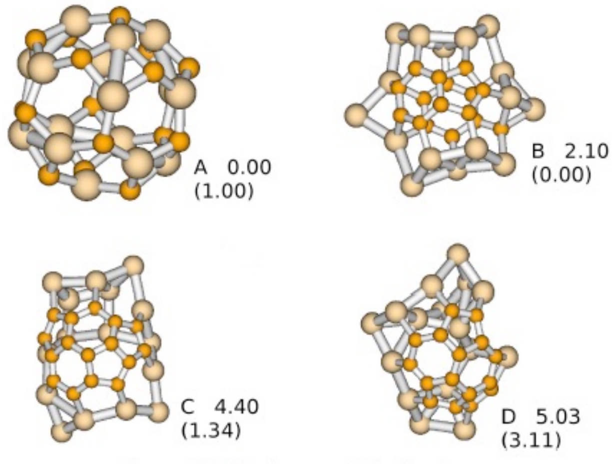

**Figure 21.** Stable isomers of $Si_{16}C_{16}$ clusters.

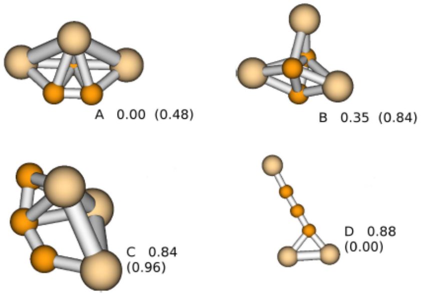

**Figure 4.** The most stable $Si_3C_3$ clusters and relative energies (in eV).

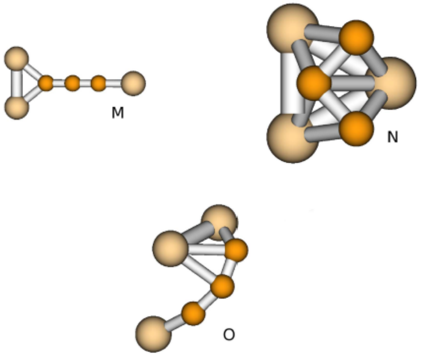

**Figure 5.** Transition states of $Si_3C_3$ clusters.

Proposed nucleation path $Si_nC_n+SiC \Rightarrow Si_{n+1}C_{n+1}$

Alternative paths $Si_nC_m+SiC_2/Si_2C=Si_{n+1}C_{m+2}/Si_{m+2}C_{n+1}$

**And why not $Si_nC_m$ + Si or + C or + $C_2$ or + $Si_n$ or + $C_n$ ???**

# Interest of IRC +10216

- Prototype of mass-lossing C-rich AGB star

- Possibility to produce detailed studies of mass loss process in AGB stars and dust formation

- Most tan 50% of known molecules in space have been detected this circumstellar envelope (all carbon radicals, all anions, all metal-bearing species –halides and cyanides-)

- Excellent laboratory to test chemical models

# The different zones for carbon chemistry

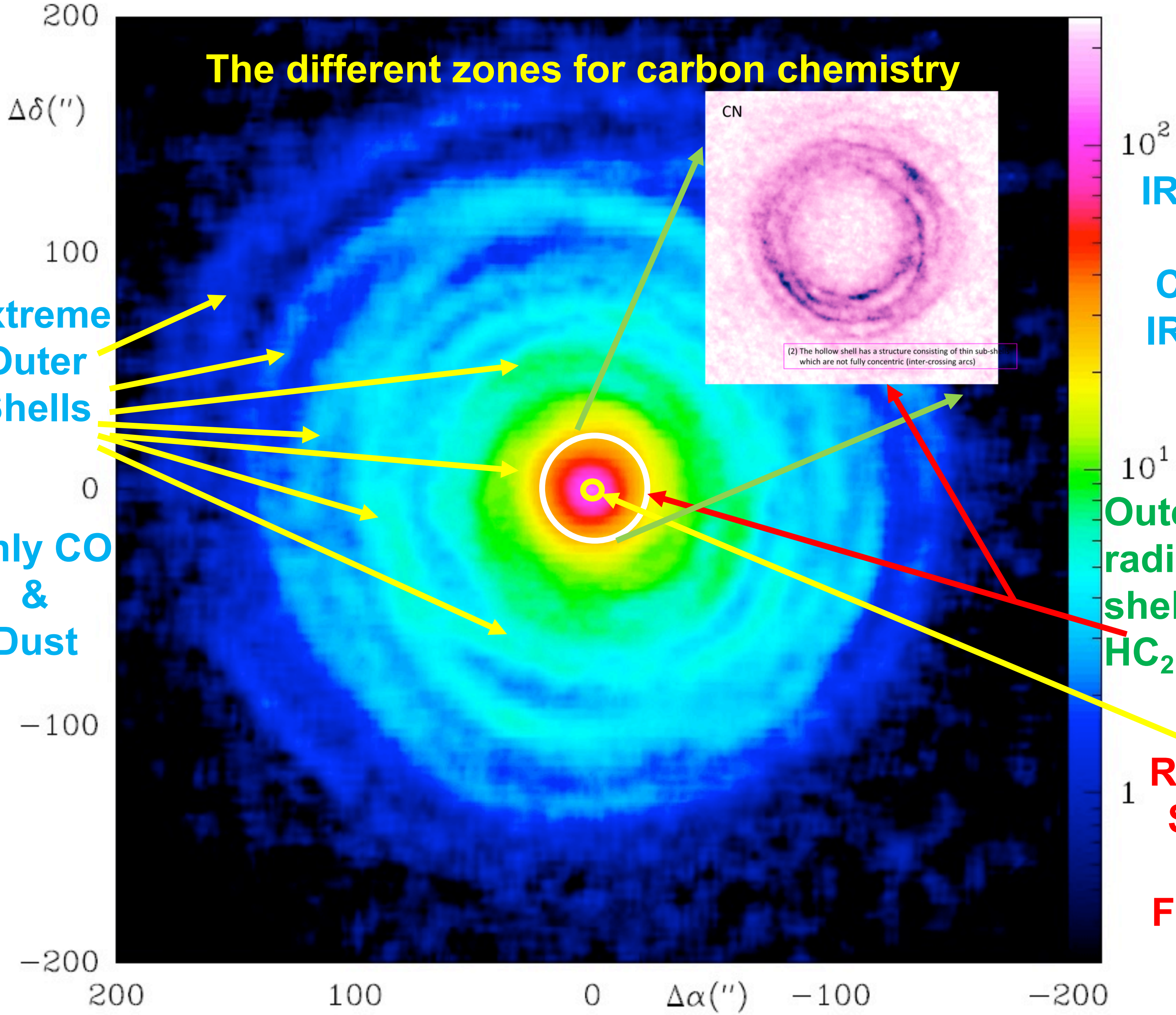

(2) The hollow shell has a structure consisting of thin sub-shells which are not fully concentric (inter-crossing arcs)

**IRC+10216**

**CO J=2-1 IRAM 30m data**

**Extreme Outer Shells**

**Only CO & Dust**

**Outer carbon radicals shell ($C_nH$, $HC_{2n+1}N$,..)**

**Inner Refractory Species. Dust Formation Zone**

Figure 1: IRC+10216 at a distance of 100 pc

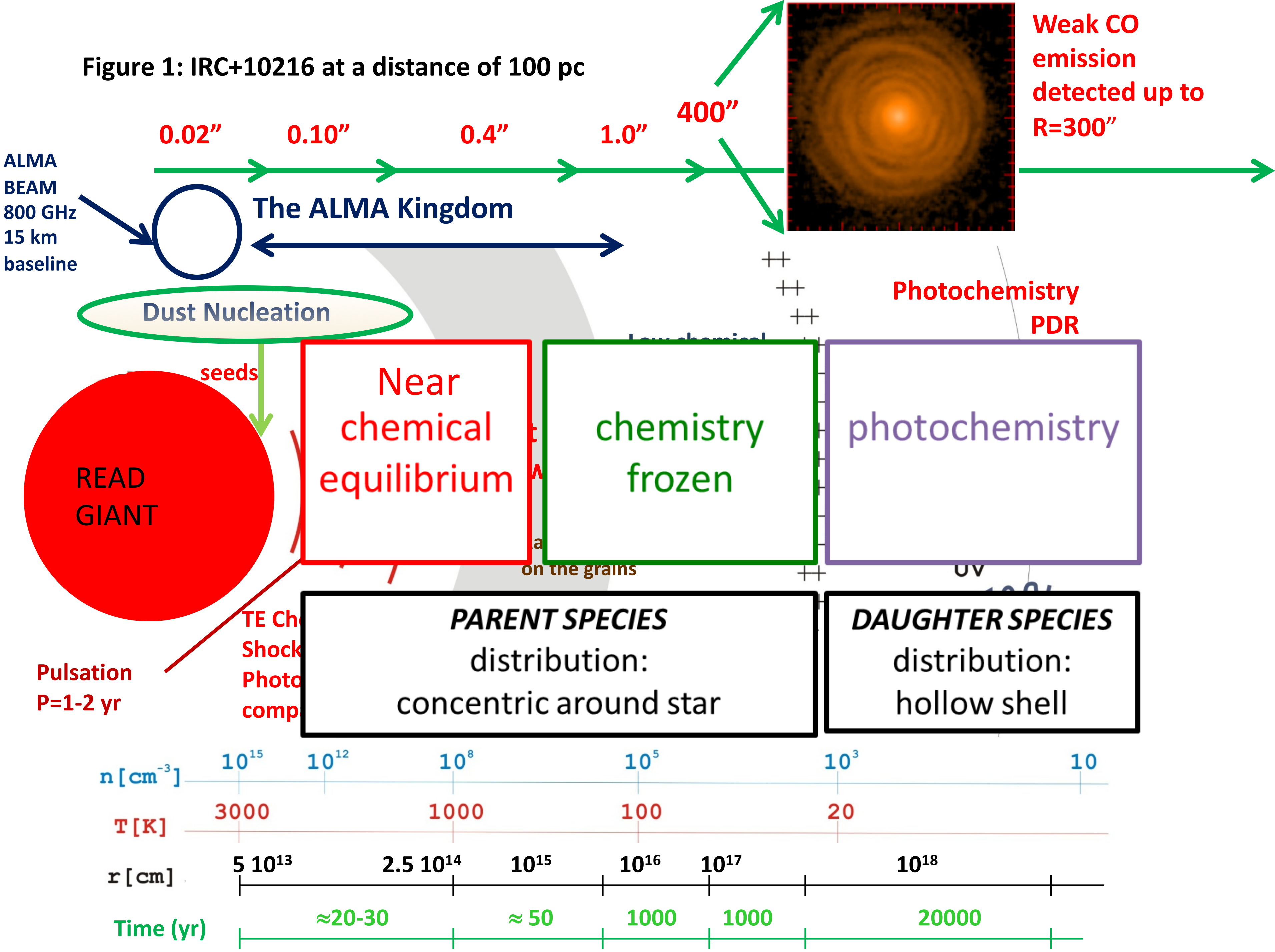

0.02” 0.10” 0.4” 1.0” 400”

Weak CO emission detected up to R=300”

ALMA BEAM 800 GHz 15 km baseline

The ALMA Kingdom

Dust Nucleation

seeds

READ GIANT

Pulsation P=1-2 yr

TE Ch
Shock
Photo
comp

Near chemical equilibrium

chemistry frozen

photochemistry

Photochemistry PDR

on the grains

UV

*PARENT SPECIES* distribution: concentric around star

*DAUGHTER SPECIES* distribution: hollow shell

| | | | | | | | | |
|---|---|---|---|---|---|---|---|---|
| n [cm$^{-3}$] | $10^{15}$ | $10^{12}$ | $10^{8}$ | | $10^{5}$ | | $10^{3}$ | 10 |
| T [K] | 3000 | | 1000 | | 100 | | 20 | |
| r [cm] | 5 $10^{13}$ | | 2.5 $10^{14}$ | $10^{15}$ | $10^{16}$ | $10^{17}$ | $10^{18}$ | |
| Time (yr) | ≈20-30 | | ≈ 50 | | 1000 | 1000 | 20000 | |

To study the dust component we need infrared observations to characterize its physical properties and its chemical composition (from spectral features)

Dust is formed from atoms and molecules: A complete characterization of the molecular content of the star and its circumstellar envelope is needed

Astrophysical observations in the infrared to characterize molecules without permanent dipole moment : $C_2H_2$, $CH_4$, $SiH_4$, $C_2H_6$, $C_2H_4$,….

Astrophysical observations in the radio, millimeter and submillimeter domains with single dishes and interferometers to study the gas composition of the circumstellar envelope : CO, HCN, $C_nH$ radicals, $HC_nN$, SiO, SiS, $Si_2C$, $SiC_2$,….

Laboratory astrophysics experiments to simulate, at the best we can, the formation of dust

# THE IR OBSERVATIONS

- CARMENES Spectrometer, resolution 82000, coverage 0.55-1.7 μm. Very well adapted to NANOSCOSMOS goals. A few stars observed
- TEXES/EXES spectrometers 5-20 μm, resolution 75000 (one/two objects)
- VLT/CRIRES o ISHEL/IRTF, 1-5 μm, resolution 100000 (2017 IRC done) (one/two objects)

# Observations of $C_2H_2$ and HCN with TEXES at the IRTF

**PhD of J.Pablo Fonfría (Fonfría et al., 2008, ApJ)**

**TEXES::Lacy et al., 2002, PASP, 114, 153**

720-900 $cm^{-1}$
11.1-13.9 μm

Spectral resolution 75000
4 km/s (0.008 $cm^{-1}$)

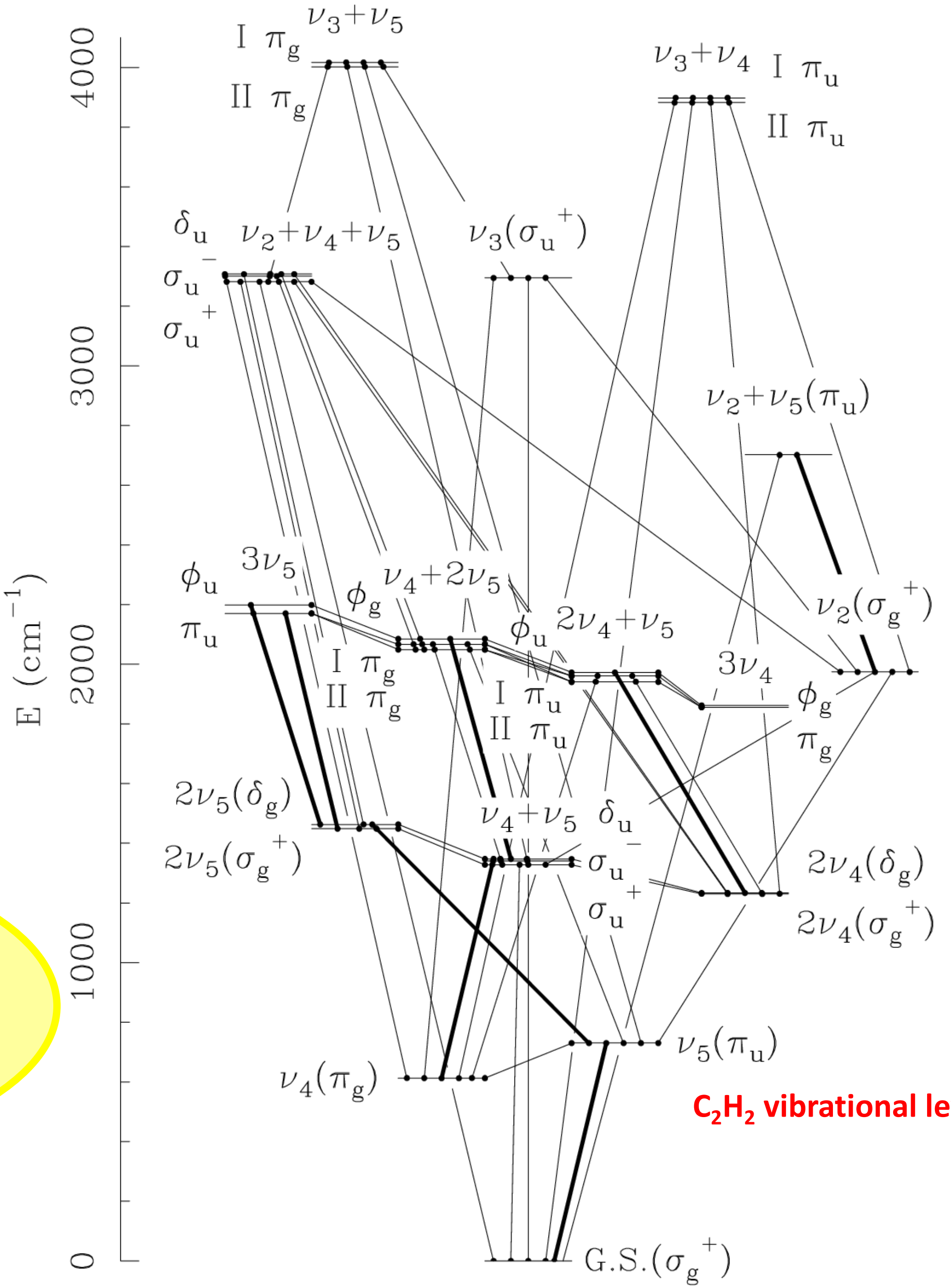

$C_2H_2$ vibrational levels

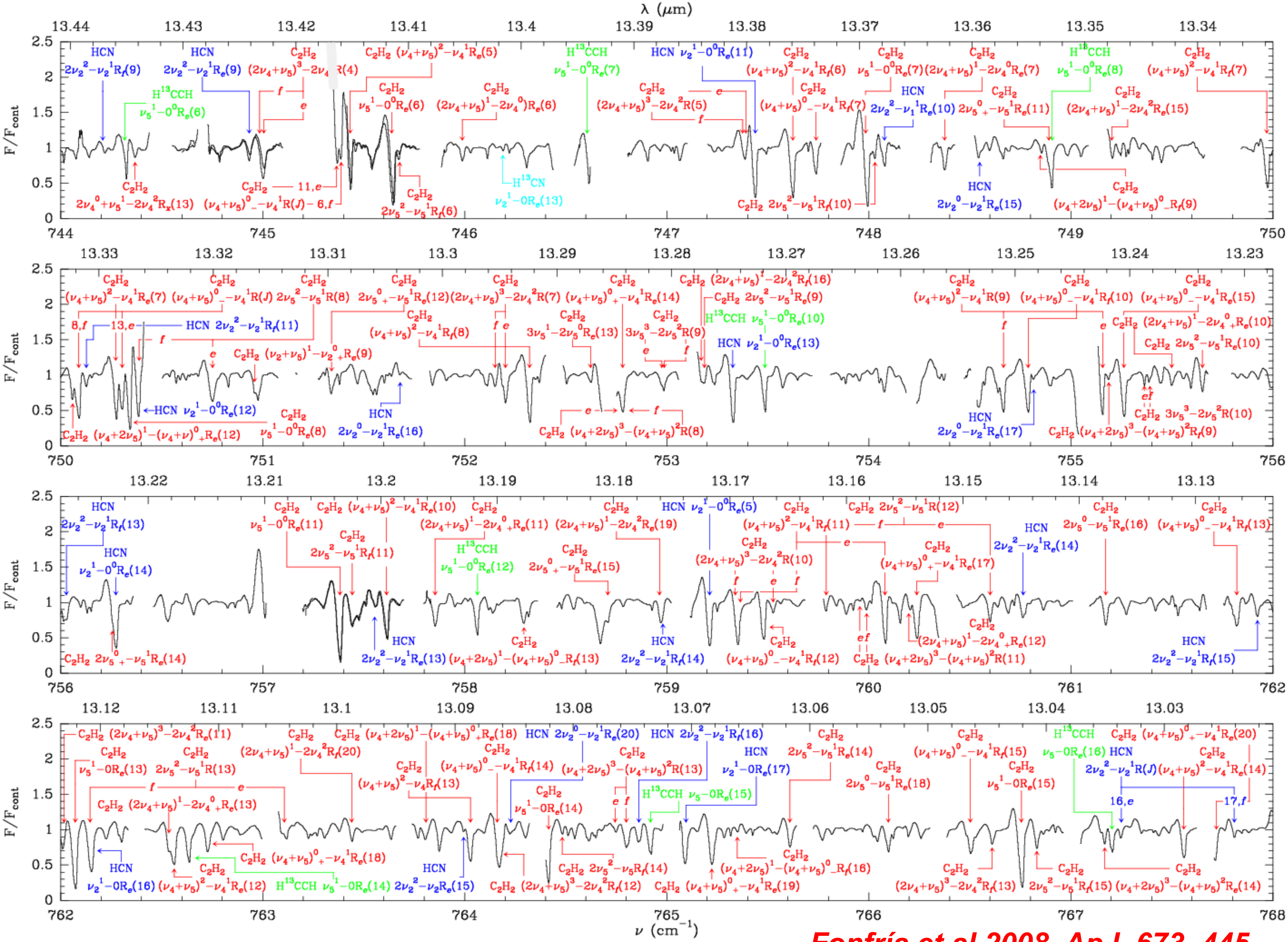

***Fonfría et al 2008, ApJ, 673, 445***

*Fonfría et al 2008, ApJ, 673, 445*

# RESULTS

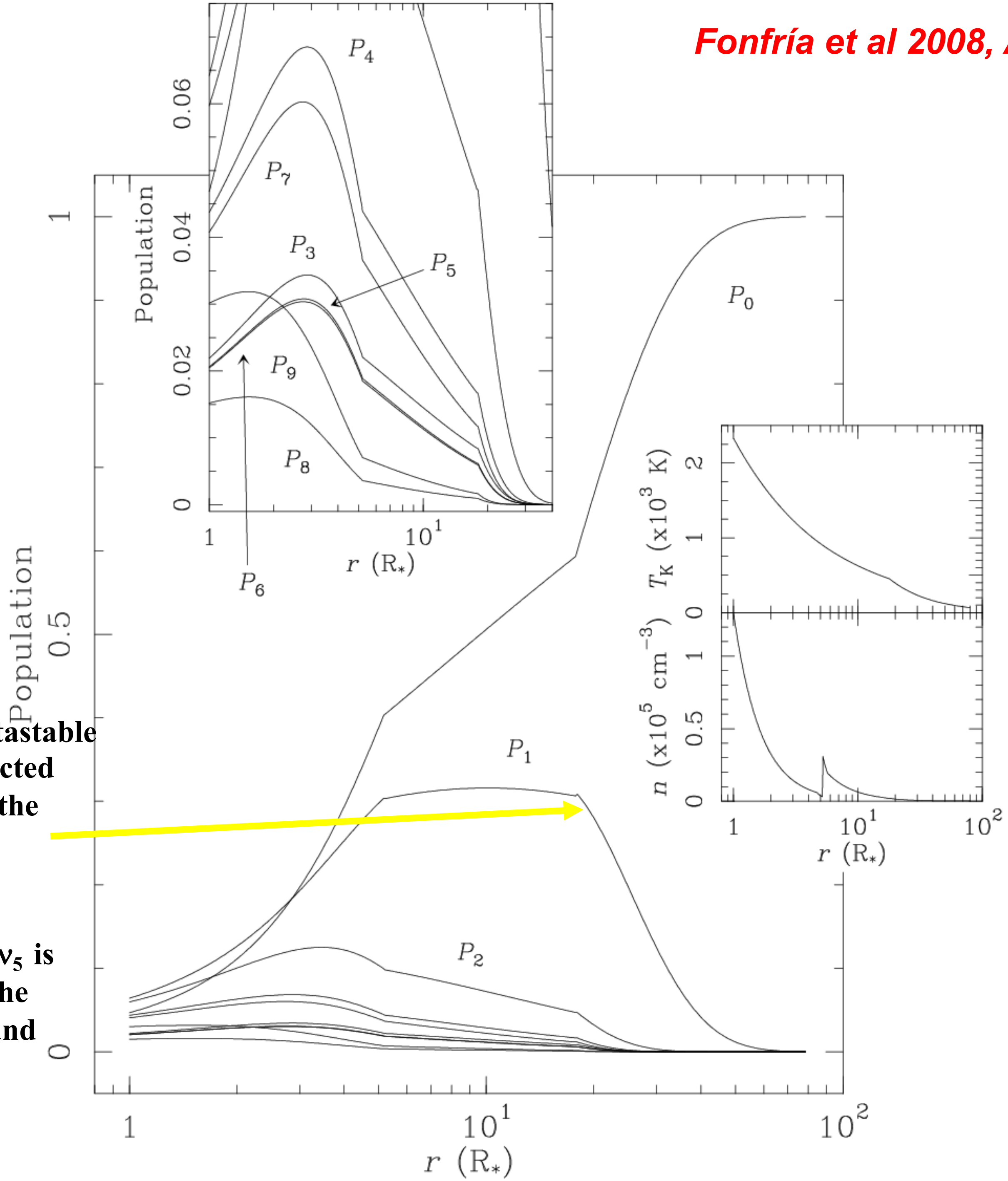

**$P_1$ ($\nu_4$) is a metastable level no connected radiatively to the ground state**

**However, $\nu_4+\nu_5$ is connected to the ground state and $\nu_4+\nu_5 \Rightarrow \nu_4$**

**x($C_2H_2$)**

| | |
|---|---|
| **Z I** | **7.5 $10^{-6}$** |
| **Z II** | **8.0 $10^{-5}$** |
| **ZIII** | **8.0 $10^{-5}$** |

**x(HCN)**

| | |
|---|---|
| **Z I** | **2.5 $10^{-5}$** |
| **Z II** | **5.0 $10^{-5}$** |
| **ZIII** | **5.0 $10^{-5}$** |

**$^{12}C/^{13}C$=41**

| | |
|---|---|
| **Z I** | **1- 5 $R_*$** |
| **Z II** | **5-20 $R_*$** |
| **ZIII** | **> 20 $R_*$** |

# $C_4H_2$ in IRC+10216 (Fonfría et al., 2017)

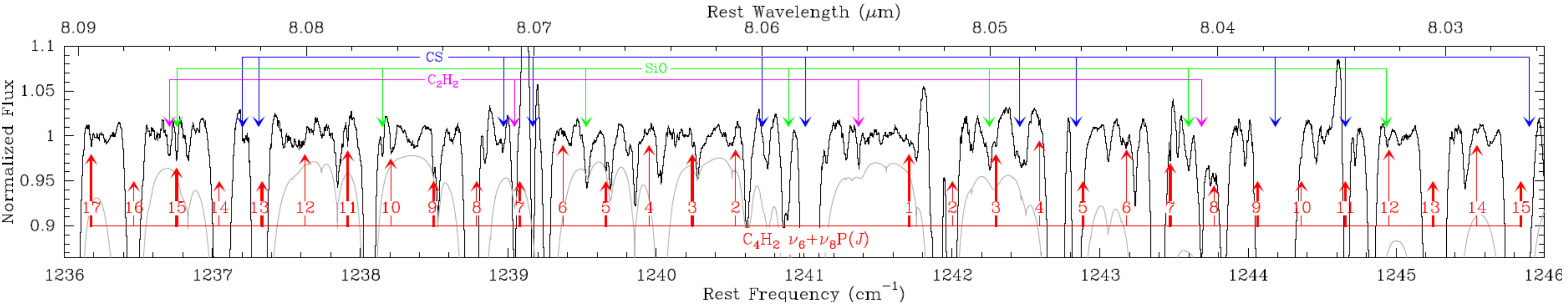

EXES observations with SOFIA.
Spectral resolution $10^5$

No traces of very warm $C_4H_2$

Formed at distances >20 R*

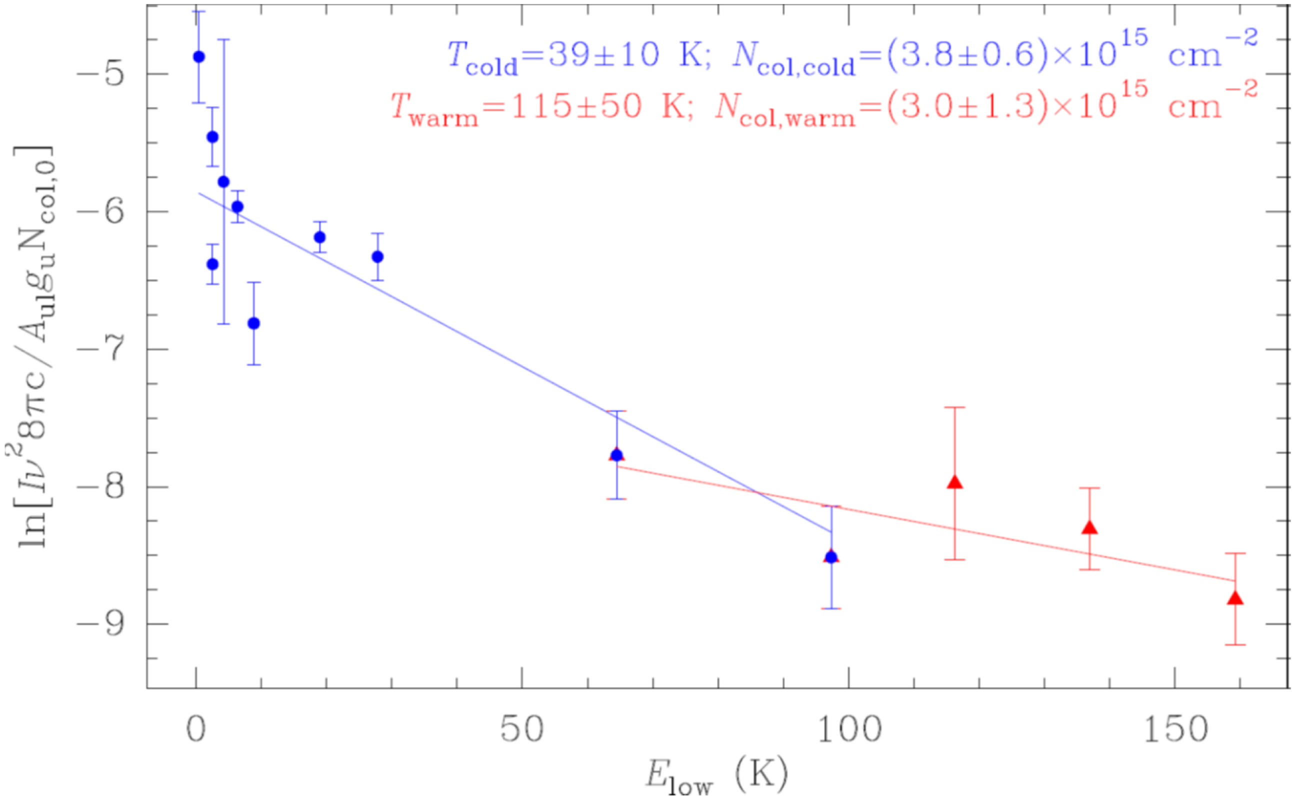

# $C_2H_4$

Fonfria et al. (2017, ApJ, 835, 196)

**Formed at distances ~20R$_*$**

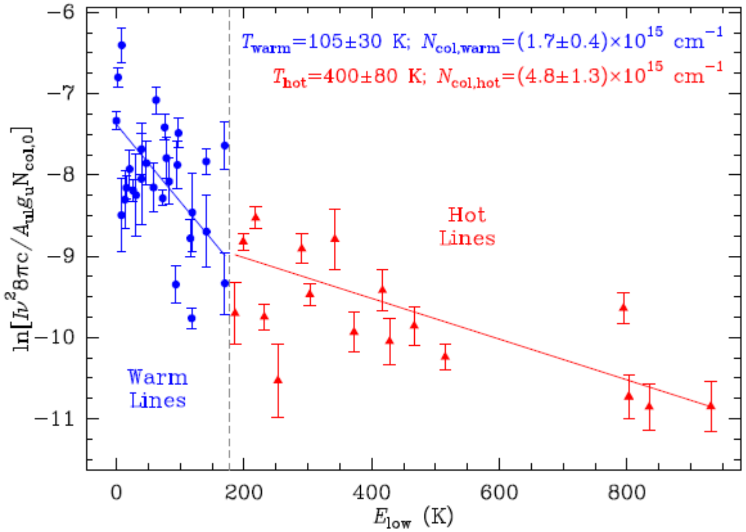

FIG. 2.— Ro-vibrational diagram of the observed $C_2H_4$ lines. The lines are separated into two different groups: warm lines (blue dots) and hot lines (red triangles). The warm lines are those involving lower ro-vibrational levels with energies below 177 K. The hot lines involve lower levels with higher energies. These groups of lines were linearly fitted separately following Eq. 2 to derive their rotational temperatures, $T_{\rm rot}$, and their column densities, $N_{\rm col}$.

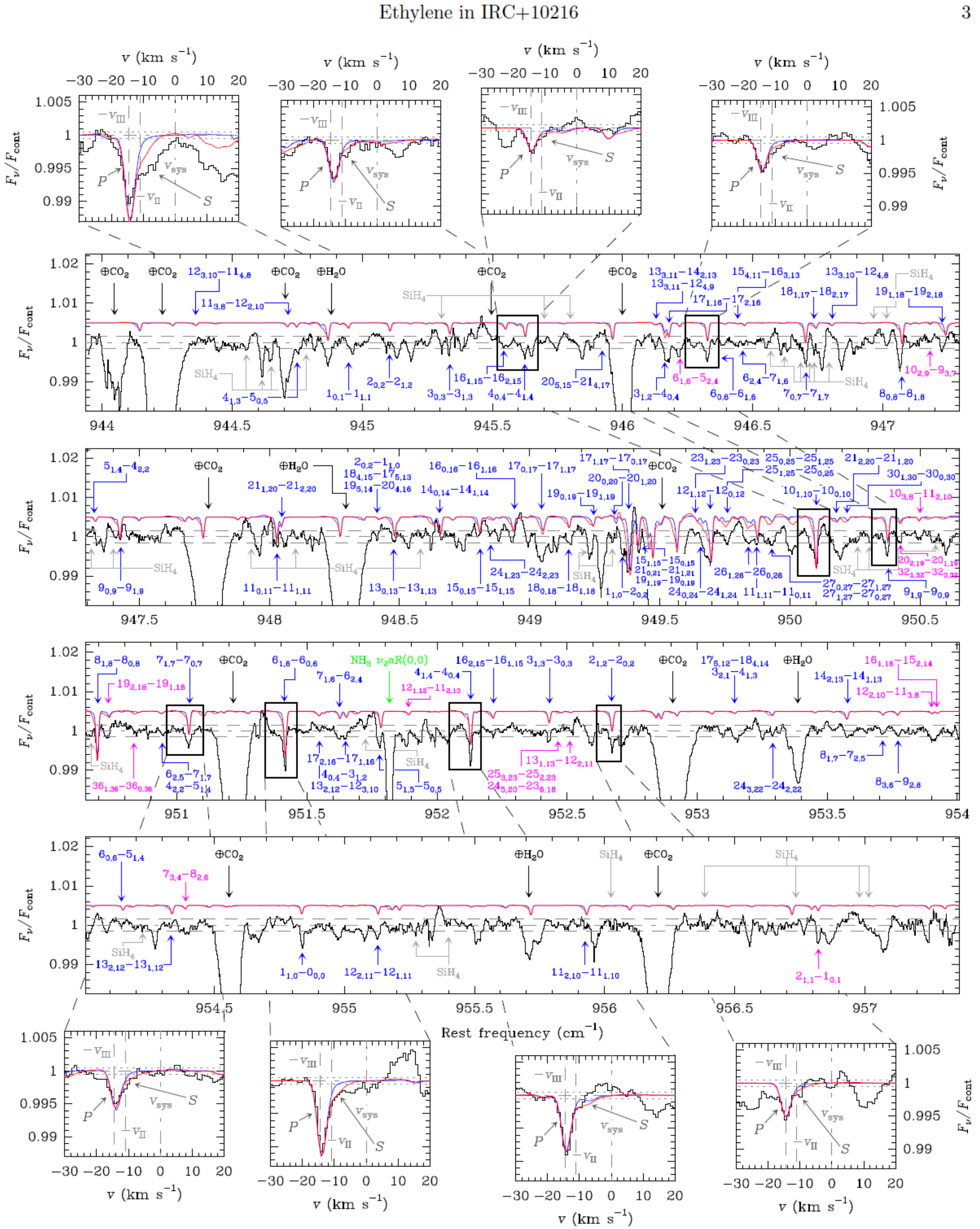

THE ASTROPHYSICAL JOURNAL, 401:269–287, 1992 December 10

# POLYCYCLIC AROMATIC HYDROCARBON FORMATION IN CARBON-RICH STELLAR ENVELOPES

ISABELLE CHERCHNEFF,[1,2] JOHN R. BARKER,[1,4] AND ALEXANDER G. G. M. TIELENS[3]

*Received 1992 January 20; accepted 1992 June 15*

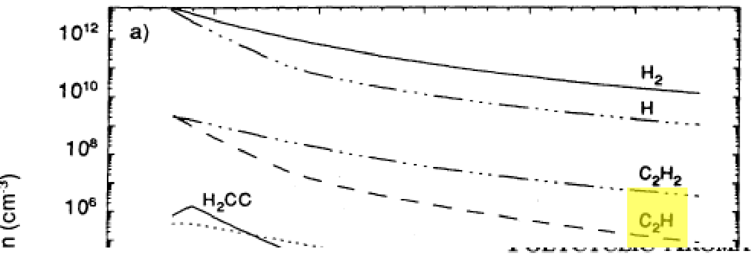

Chemical network based on Frenklach and Feigelson (1989, ApJ, 341, 372) with some modifications. Uses the vynilidene cumulenic isomer of acetylene (**$H_2C_2$ has a very short live; it is not a good precursor**)

| Number | Reaction[a] | Rate Coefficient[b] A | n | $E_a$ (kJ mole$^{-1}$) |
|---|---|---|---|---|
| (R1) ..................... | $H + H + H_2 = H_2 + H_2$ | 2.67 (−31) | −0.6 | |
| (R2) ..................... | $C_2H_2 + M = C_2H + H + M$ | 6.97 (−8) | | 448 |
| (R3) ..................... | $C_2H_2 + M = H_2CC + M$ | 5.31 (−8) | | 159 |
| (R4) ..................... | $H_2CC + C_2H_2 \rightarrow C_4H_4$ | 5.31 (−12) | | 8.4 |
| (R5) ..................... | $C_4H_4 + M \rightarrow C_2H_2 + C_2H_2 + M$ | 4.48 (−7) | | 266 |
| (R6) ..................... | $C_4H_4 + M = C_4H_2 + H_2 + M$ | 4.48 (−8) | | 266 |
| (R7) ..................... | $H_2CC + H_2 \rightarrow C_2H_3 + H$ | 3.32 (−11) | | 80 |
| (R8) ..................... | $C_2H_3 + H \rightarrow H_2CC + H_2$ | 2.49 (−11) | | |

photos-
t distro-
ey are
oscillato-
gh densities
reach or
approach equilibrium again.

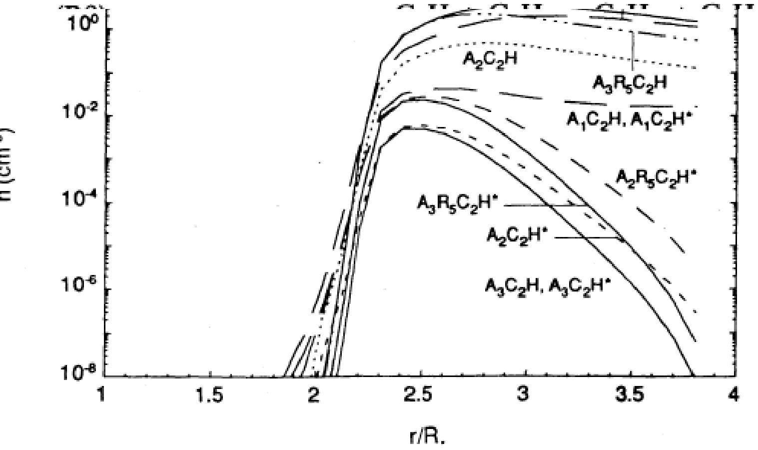

FIG. 7.—Concentration profiles for case 2: (*a*) main hydrocarbon molecules; (*b*) aromatic radicals and molecules.

So far the most complete modelling of the formation of PAHs (up to $C_{18}H_{12}$). Even if shocks are present the yield of PAHs is moderate.

There is a possibility to check the models (new models):
- Looking for molecules predicted by the calculations
- Analyzing the line profiles for the presence of shocks

THE ASTROPHYSICAL JOURNAL, 546:L123–L126, 2001 January 10

# *INFRARED SPACE OBSERVATORY'S* DISCOVERY OF $C_4H_2$, $C_6H_2$, AND BENZENE IN CRL 618

JOSÉ CERNICHARO,[1,2] ANA M. HERAS,[3] A. G. G. M. TIELENS,[4] JUAN R. PARDO,[1,5] FABRICE HERPIN,[1]
MICHEL GUÉLIN,[6] AND L. B. F. M. WATERS[7]

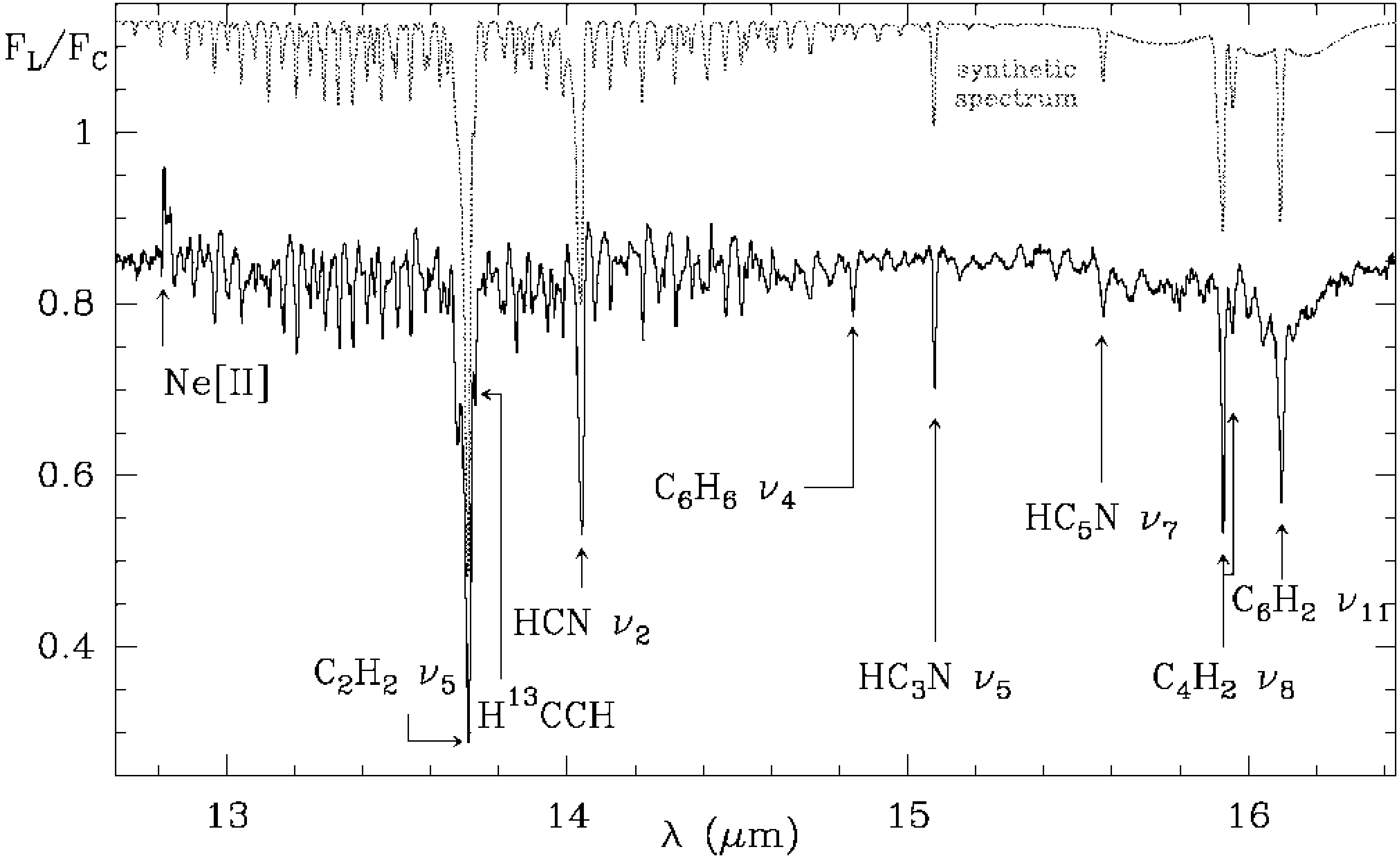

THE ASTROPHYSICAL JOURNAL, 546:L127–L130, 2001 January 10

# METHYLPOLYYNES AND SMALL HYDROCARBONS IN CRL 618

JOSÉ CERNICHARO,[1,2] ANA M. HERAS,[3] JUAN R. PARDO,[1,4] A. G. G. M. TIELENS,[5] MICHEL GUÉLIN,[6]
E. DARTOIS,[6] R. NERI,[6] AND L. B. F. M. WATERS[7]

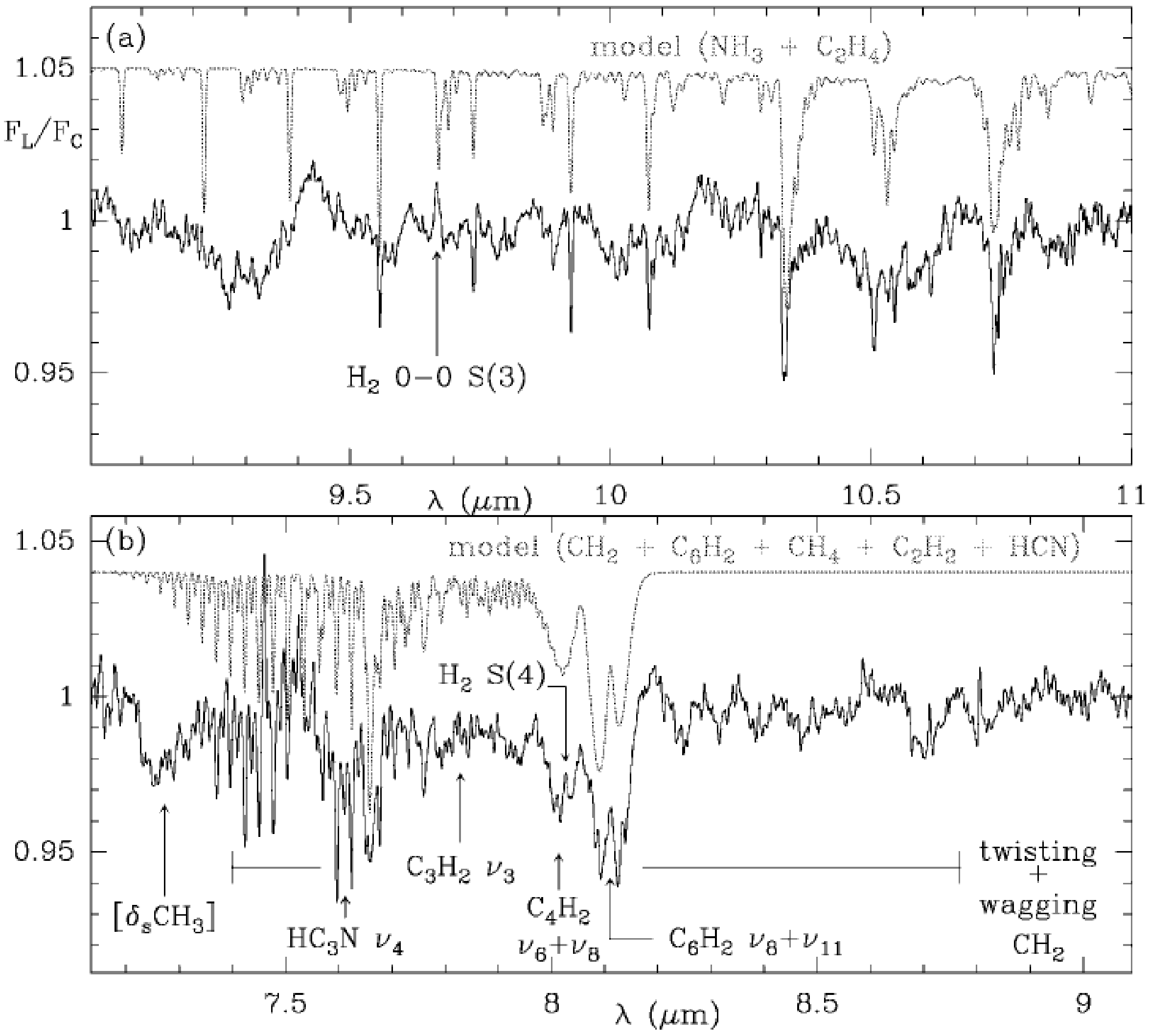

Aliphatic matter !!!

See Cernicharo 2004, ApJ, 608, L41 for a photochemical study of this object and the role of $H_2$+$C_nH$ reactions !

Polymerization of HCN and $C_2H_2$ => very large abundances of polyacetylene and cyanopolyyne molecules.

$HC_3N$ and $HC_5N$ are enhanced by a factor 100 with respect AGB abundances.

Some, but minor, yield of benzene

# The chemistry of carbon in AGBs outside thermodynamical equilibrium

- Key termolecular reactions (from atoms to diatomics A+B+M=>AB+M):
  C + C + M =>$C_2(^1\Sigma)/C_2(^3\Pi)$; $\tau(C_2(^3\Pi))$=120 μs; Energy($C_2(^3\Pi)$)=716 $cm^{-1}$

- $C_2(^1\Sigma)$+M = $C_2(^3\Pi)$ (the triplet state is detected in the photosphere of all carbon stars). At 2000 K $C_2(^3\Pi)/C_2(^1\Sigma)\sim5$.

- $C_2$+C+M=$C_3$ and so on ($C_n$+$C_m$+M) but it takes time to grow and clusters could react with other species (H, $H_2$, metals) to form hydrocarbons (mainly acetylene, but also $C_nH_m$ species). **Time becomes a real limitation for the growth of clusters.**

- Reactions involving $H_2$ and radicals can be faster than 3-body reactions at 1000-1500 K for n($H_2$)<$10^{10}$ $cm^{-3}$ ($H_2$+$C_2$ ($^1\Sigma$)=>CCH + H; $H_2$+CCH=>$C_2H_2$+H). They have to be included in any reasonable model. **Moreover, $H_2$ in v=1 is highly abundant (much more than any other element or molecule).** These reactions become also crucial in the protoplanetary nebula phase where photochemistry is the driving mechanism for molecular growth

  (Cernicharo 2004, ApJ, 608, L41)

# The chemistry of carbon in AGBs outside thermodynamical equilibrium

- The problem of bimolecular reactions of SMALL carbon clusters: $C_n$ with n **even** have **triplet** states, but with n **odd** they have **singlet** states. Hence the radiative association $C_n+C_{n+1} = C_{2n+1}$ is spin forbidden !!!! (for n < 9-10 when clusters become ring-shaped)

- In principle $C_2+C_2 = C_3 + C(^3P)$ is spin forbidden if the two $C_2$ are in the singlet state. **However, the reaction is spin allowed if at least one of them is in the triplet state.**

- **Hence, $C_3$ could be formed if $C_2$ is not consumed by reactions with $H_2$ and $C_2(^3\Pi)$ is available.**

- **$C_2(^3\Pi)$ reacts slowly with $H_2$ but $C_2(^1\Sigma)$ reacts fast if T is high: The excitation state of molecules has to be included in our chemical kinetic models !!! (at least for sizes below ~8-10 atoms)**

# The central source (CW Leo) seen by ALMA

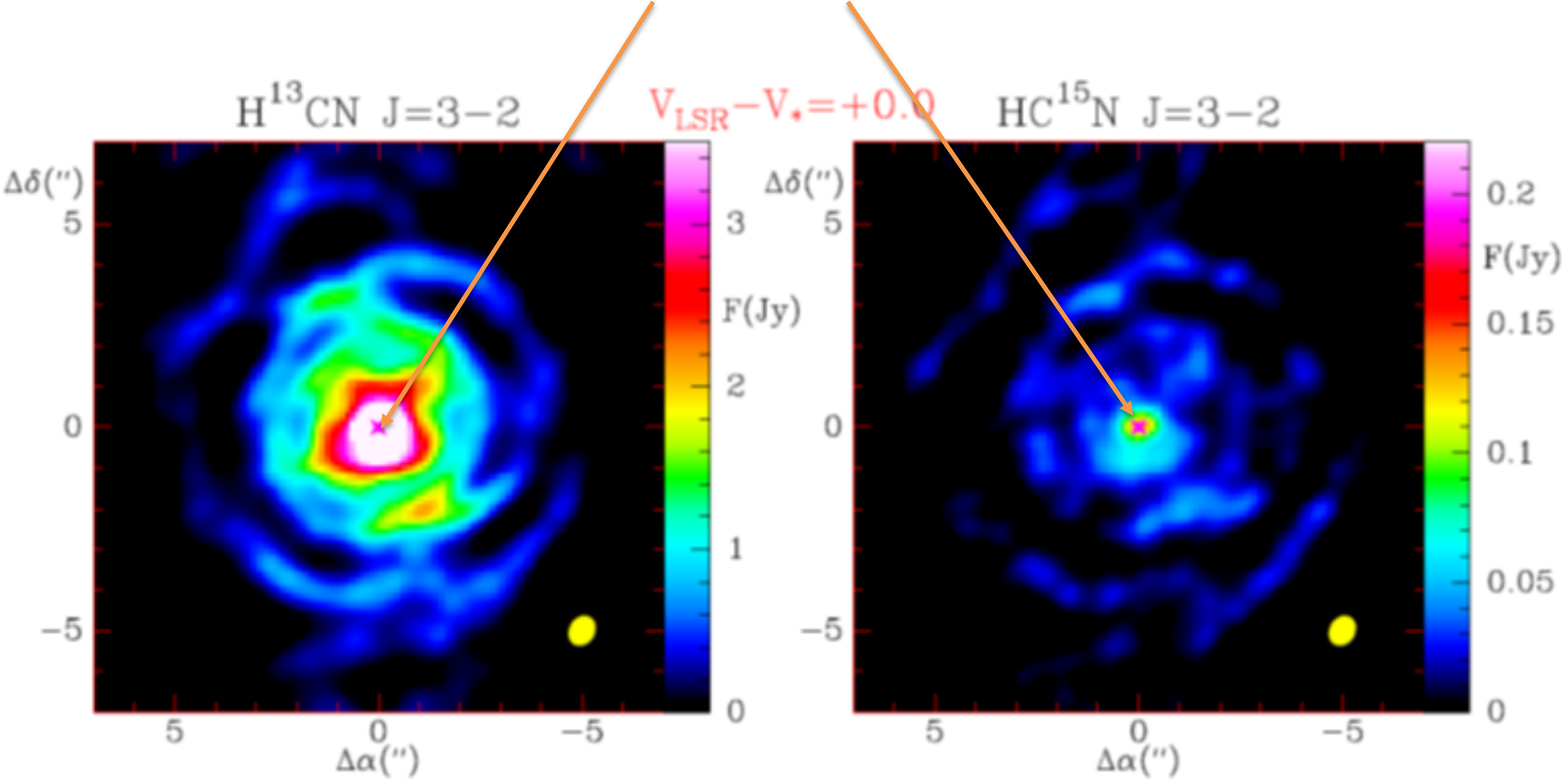

# The central source (0.6”)

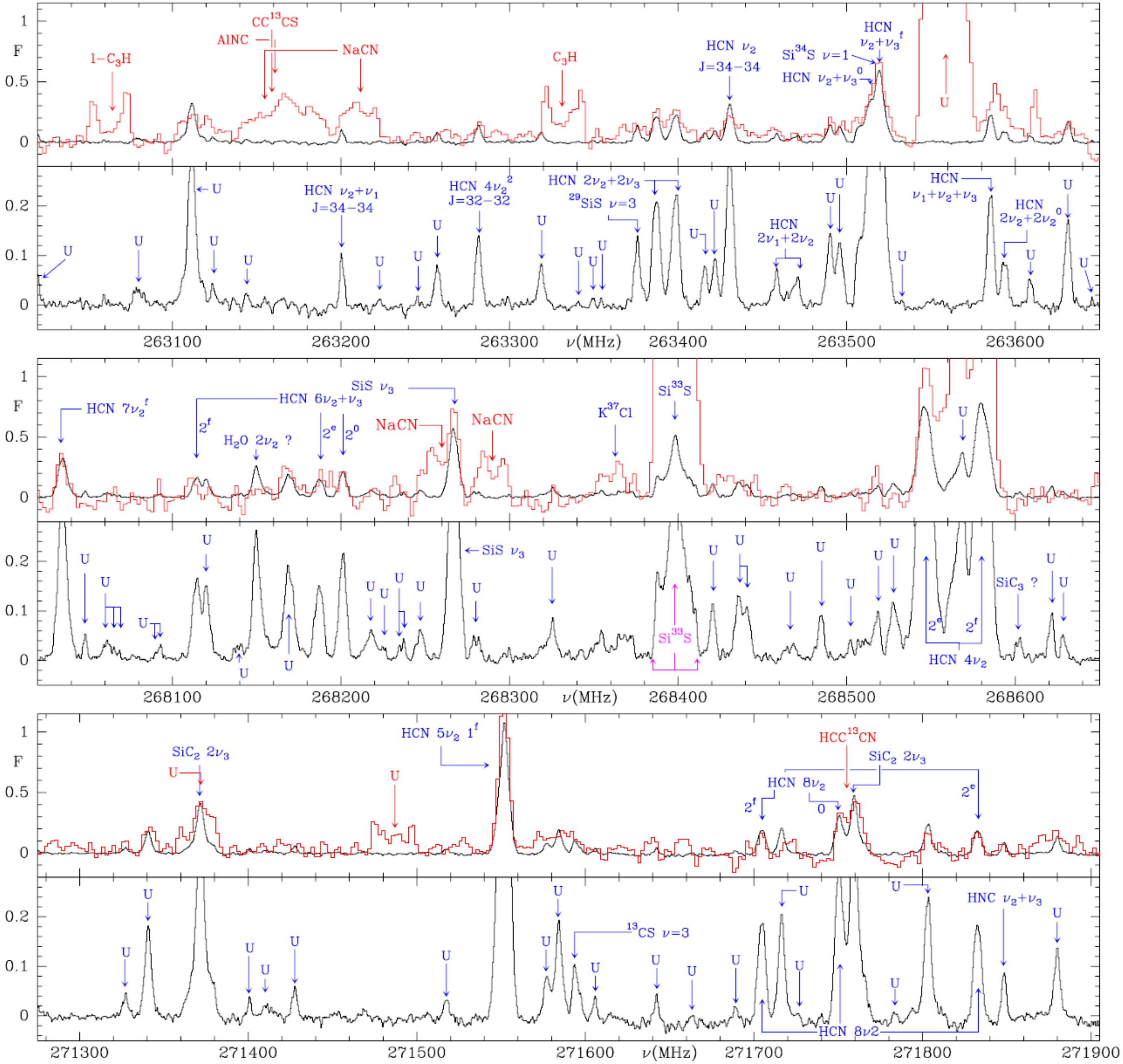

*Cernicharo et al., 2013, ApJ,778, L25*

**HCN, HNC, SiO, SiS, CS, $SiC_2$**

**HCN in all vib levels up to 16000 K ($11000$ cm$^{-1}$)**

**$H^{13}CN$ up to 8000 K**

**$H^{15}NC$ up to 5000 K**

**HNC up to vib levels ~5000 cm$^{-1}$**

**SiS up to *v*=12**

**Hundreds of U lines**

# Rotational spectroscopy of HOT HCN is really needed. Work on collaboration with J. Pearson (JPL)

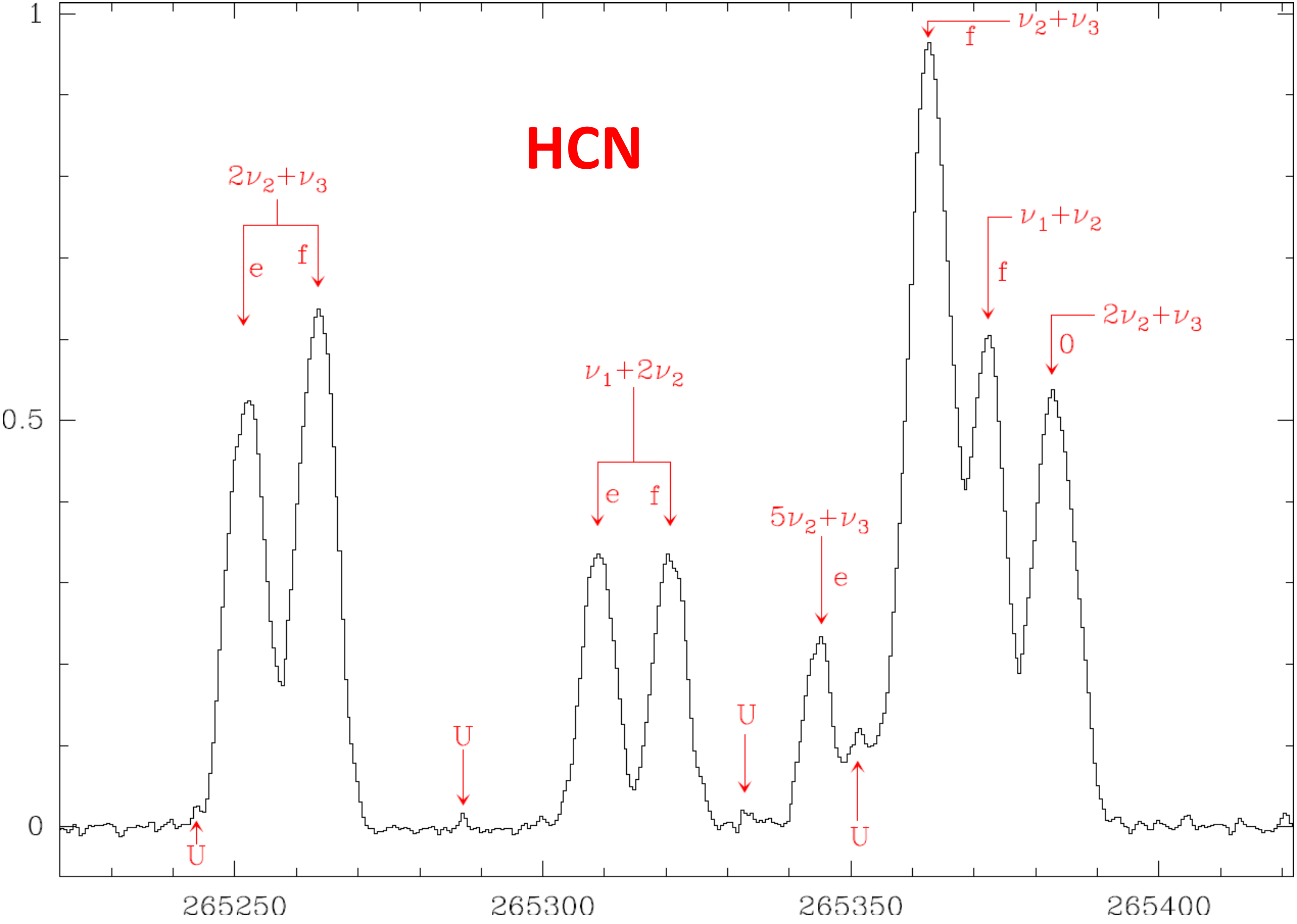

**MADEX :::** Uij for 77 diatomic molecules. 243 vibrational levels of HCN……..
by December 1st 6001 spectral entries

# Spatial distribution of vibrationally excited lines around IRC+10216

All emission is confined in a radius of 20 $R_*$

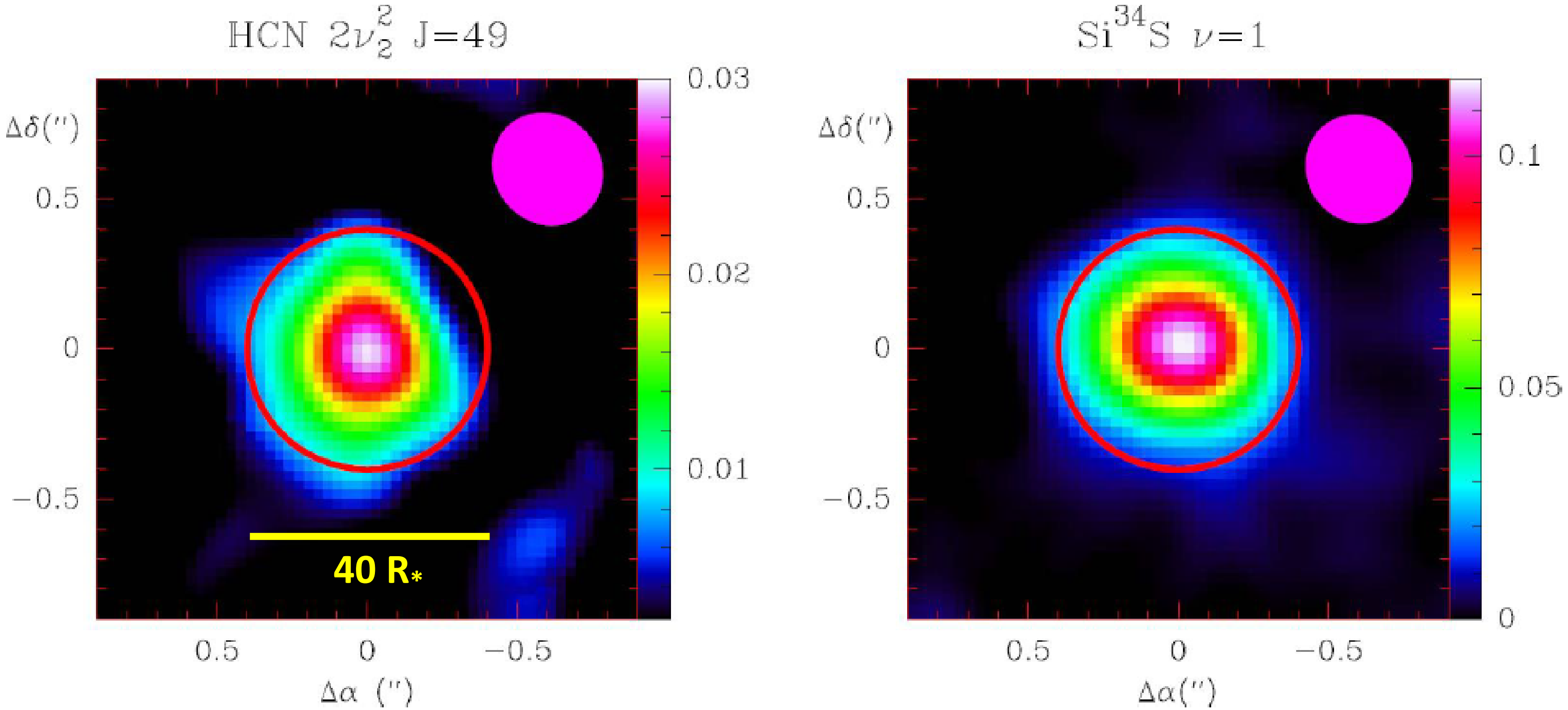

**Figure 1:** *Observed spatial distribution of some highly excited vibrational lines of HCN (a $\Delta J=0$ line with J=49 arising from $2\nu_2^2$) and Si$^{34}$S $v$=1. The red circle shows a region with a radius of 0.4", i.e., 20 stellar radii. The emission is confined to the zone inside this circle. The synthetic ALMA beam is 0.39"x0.36" for HCN and 0.37"x0.35" for Si$^{34}$S (it is indicated at the right top corner of each panel). By observing several vibrational lines of the same species it will be possible to derive the kinetic temperature of the gas and the molecular abundances. From their linewidths as a function of the position, the velocity field in the dust formation zone will also be derived. Science goal 1 will provide a map of this region of 40x40 pixels of 0.02".*

# The effect of shocks

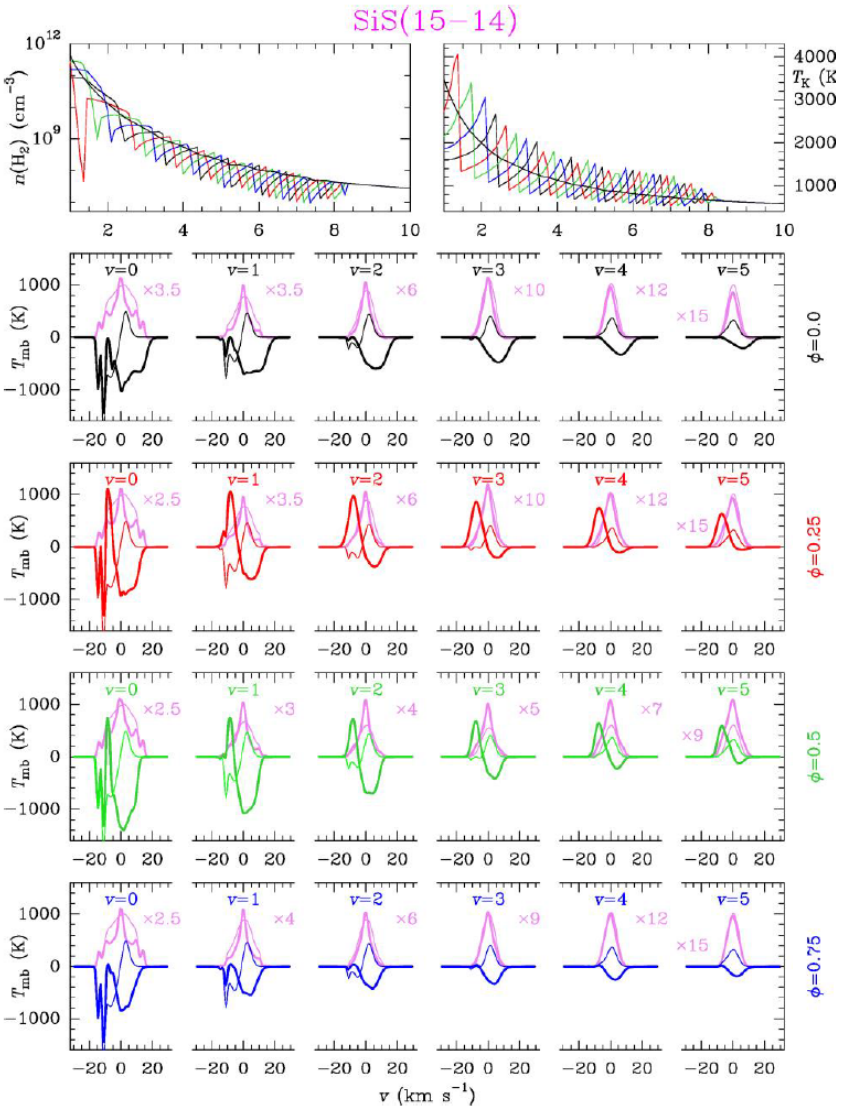

Fonfría, Cherchneff + in prep

**0.02” model with shocks** **0.6” model with shocks**

0.02” models no-shocks 0.6” model no-shocks

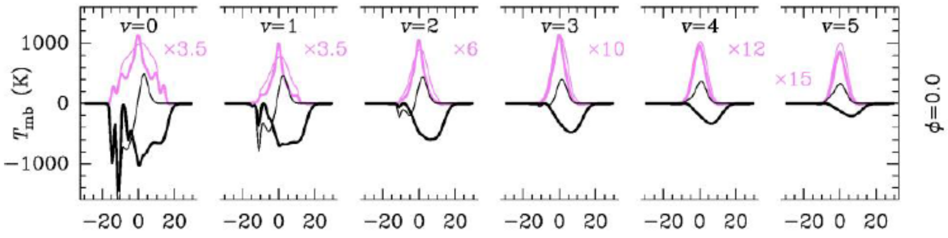

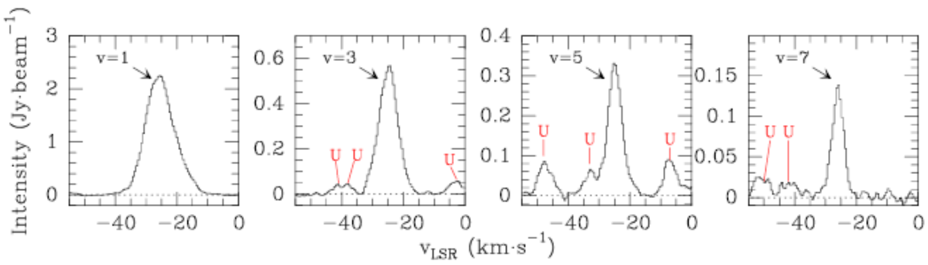

ALMA observations 0.6” resolution
Velilla-Prieto +, 2015, 805, L13
0.02” observations are coming !!!

Spatial distribution of several molecular species at the systemic velocity of the star

ALL DATA (84-116 GHz) MERGED WITH SHORT SPACINGS

➔HNC compact, extended and short spacings

Each molecule provides a different information depending of its excitation conditions and its chemistry

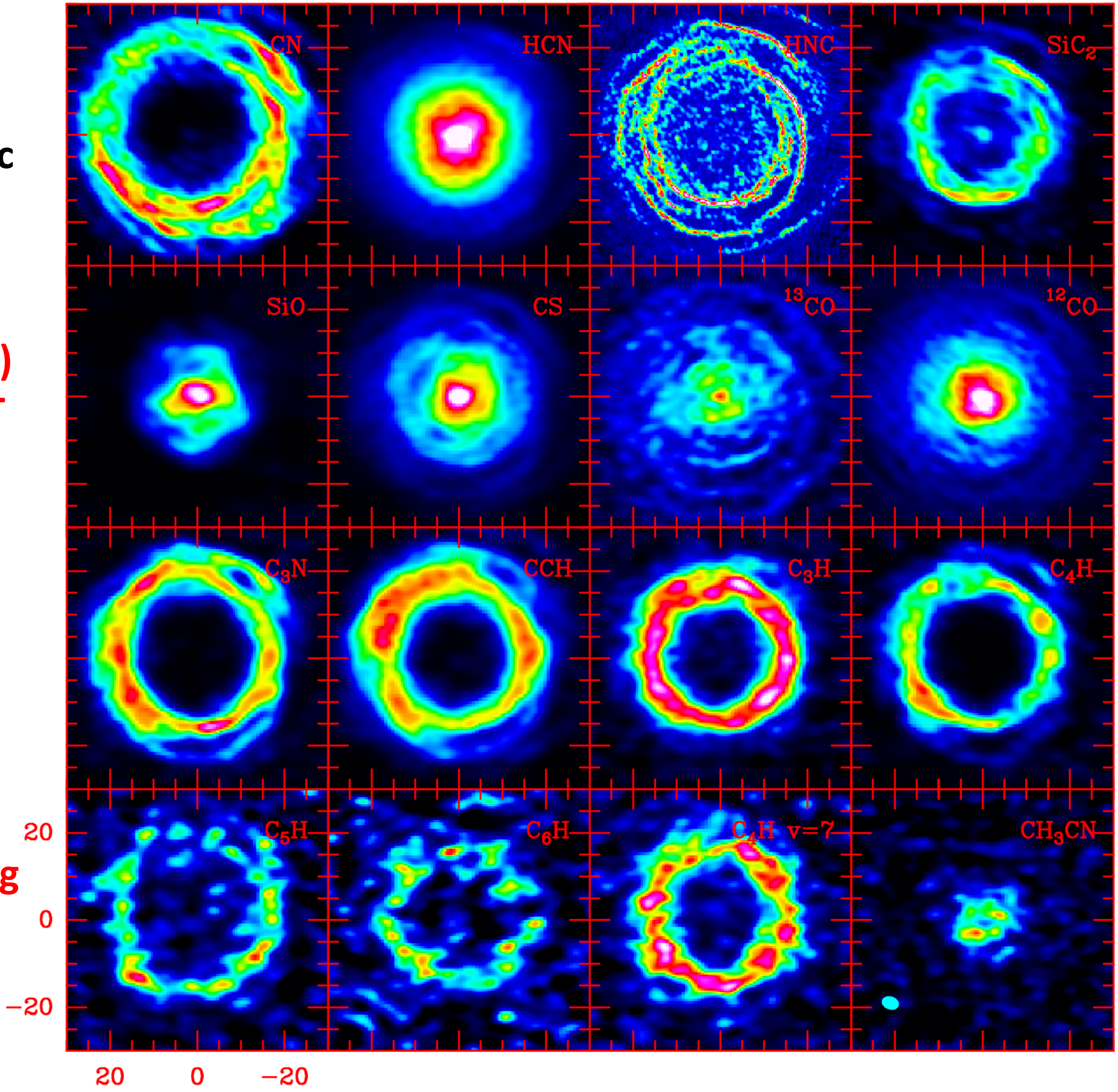

Massalkhi +, 2019, A&A, 628, A62

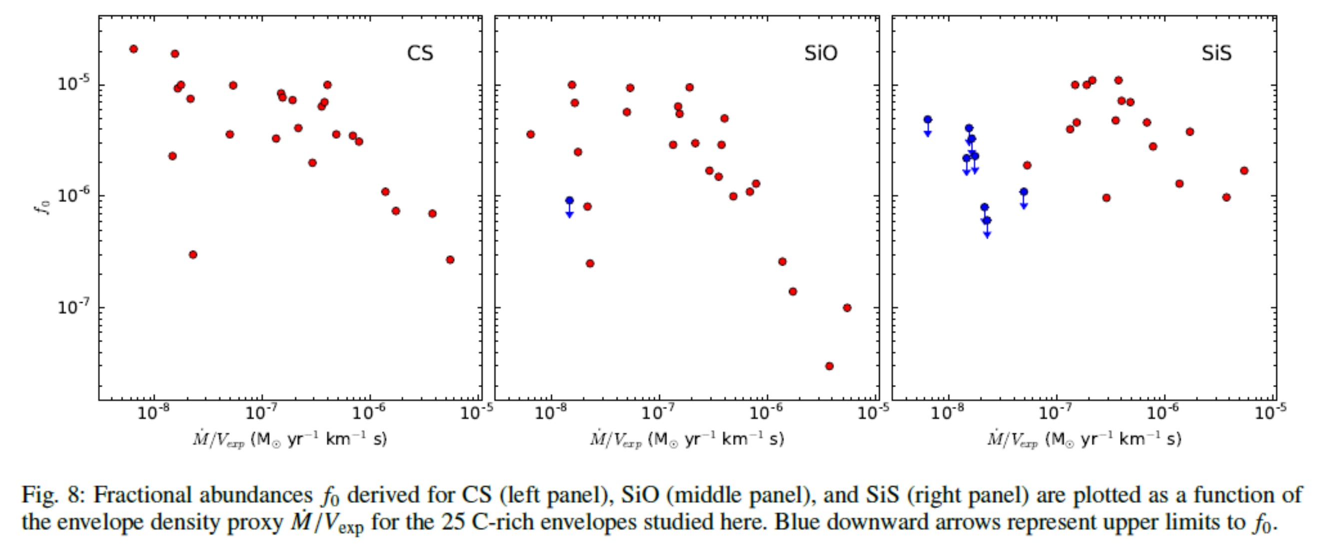

Fig. 8: Fractional abundances $f_0$ derived for CS (left panel), SiO (middle panel), and SiS (right panel) are plotted as a function of the envelope density proxy $\dot{M}/V_{\rm exp}$ for the 25 C-rich envelopes studied here. Blue downward arrows represent upper limits to $f_0$.

Massalkhi +, 2017, A&A, 611, A29

SiC$_2$ as an important Component of SiC-dust

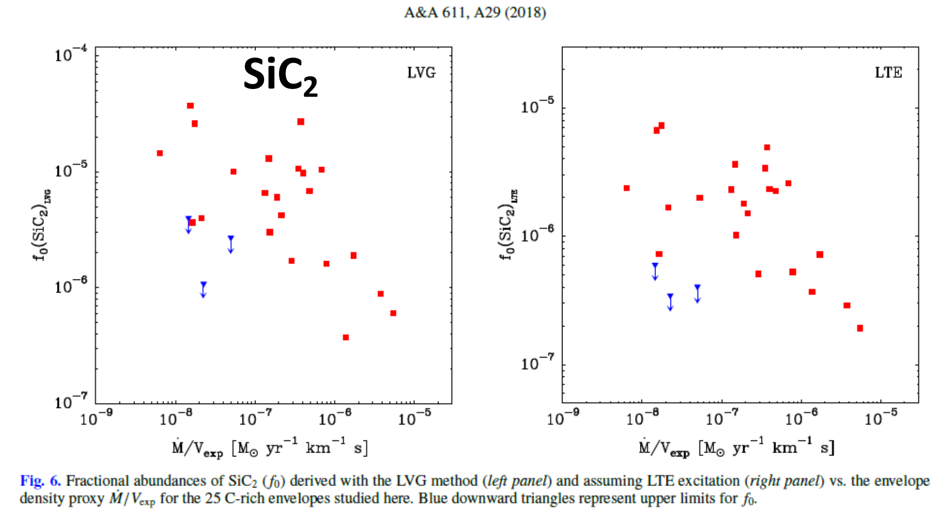
A&A 611, A29 (2018)

Fig. 6. Fractional abundances of SiC$_2$ ($f_0$) derived with the LVG method (*left panel*) and assuming LTE excitation (*right panel*) vs. the envelope density proxy $\dot{M}/V_{\rm exp}$ for the 25 C-rich envelopes studied here. Blue downward triangles represent upper limits for $f_0$.

# Velilla-Prieto +, 2019, A&A, in press

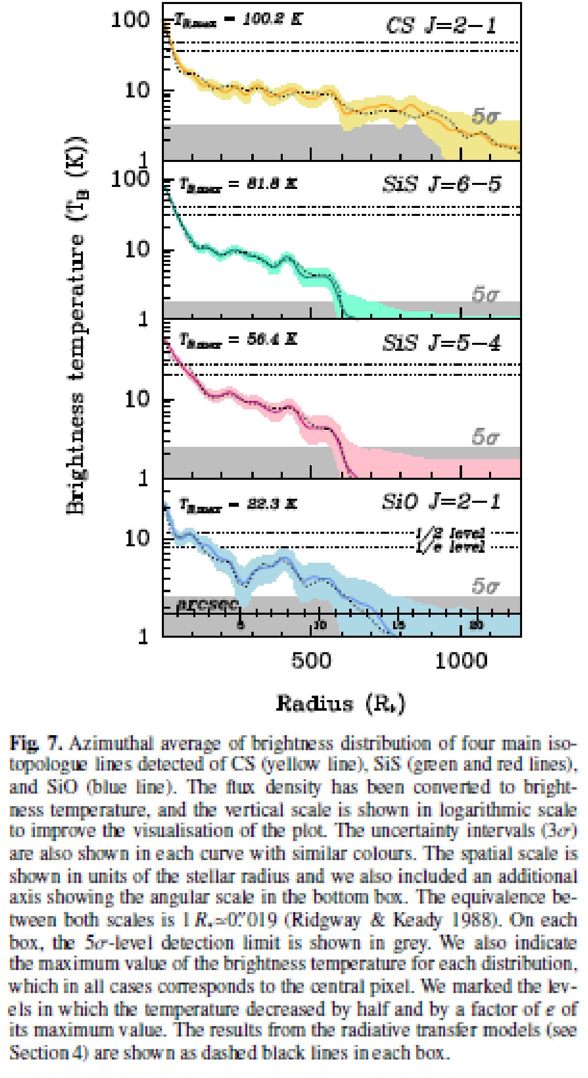

**Fig. 7.** Azimuthal average of brightness distribution of four main isotopologue lines detected of CS (yellow line), SiS (green and red lines), and SiO (blue line). The flux density has been converted to brightness temperature, and the vertical scale is shown in logarithmic scale to improve the visualisation of the plot. The uncertainty intervals ($3\sigma$) are also shown in each curve with similar colours. The spatial scale is shown in units of the stellar radius and we also included an additional axis showing the angular scale in the bottom box. The equivalence between both scales is 1 $R_*$≃0.″019 (Ridgway & Keady 1988). On each box, the $5\sigma$-level detection limit is shown in grey. We also indicate the maximum value of the brightness temperature for each distribution, which in all cases corresponds to the central pixel. We marked the levels in which the temperature decreased by half and by a factor of $e$ of its maximum value. The results from the radiative transfer models (see Section 4) are shown as dashed black lines in each box.

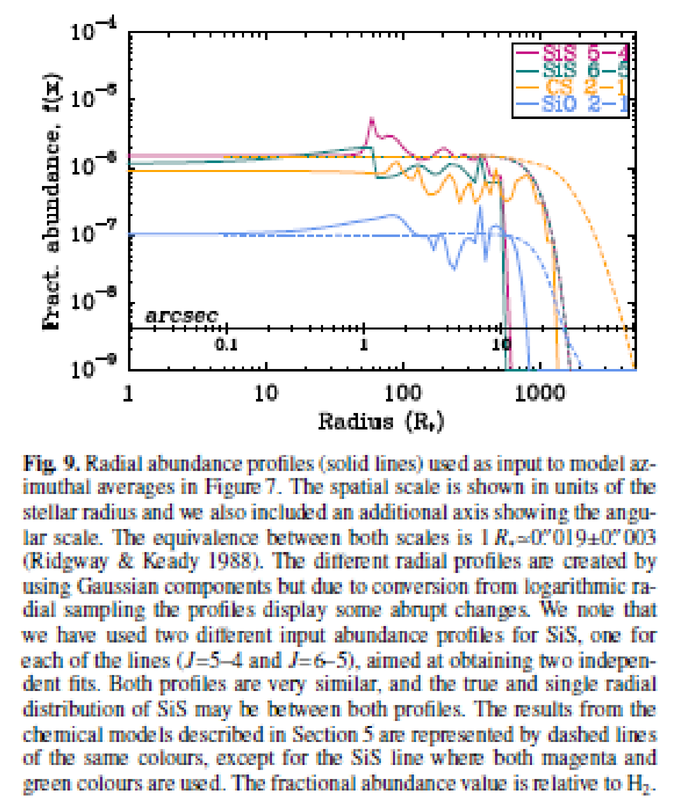

**Fig. 9.** Radial abundance profiles (solid lines) used as input to model azimuthal averages in Figure 7. The spatial scale is shown in units of the stellar radius and we also included an additional axis showing the angular scale. The equivalence between both scales is 1 $R_*$≃0.″019±0.″003 (Ridgway & Keady 1988). The different radial profiles are created by using Gaussian components but due to conversion from logarithmic radial sampling the profiles display some abrupt changes. We note that we have used two different input abundance profiles for SiS, one for each of the lines ($J$=5–4 and $J$=6–5), aimed at obtaining two independent fits. Both profiles are very similar, and the true and single radial distribution of SiS may be between both profiles. The results from the chemical models described in Section 5 are represented by dashed lines of the same colours, except for the SiS line where both magenta and green colours are used. The fractional abundance value is relative to $H_2$.

After 20 R* the abundances of SiS, SiO, CS do not suffer significant changes until the photodissociation region

Gas and dust becomes well decoupled at 20 R*

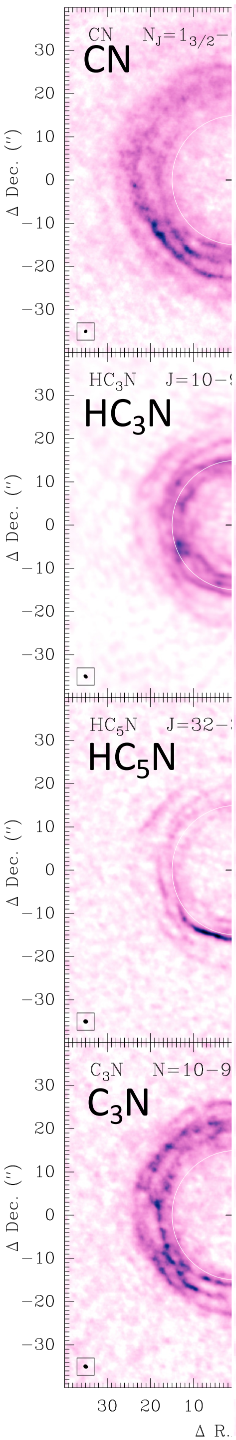

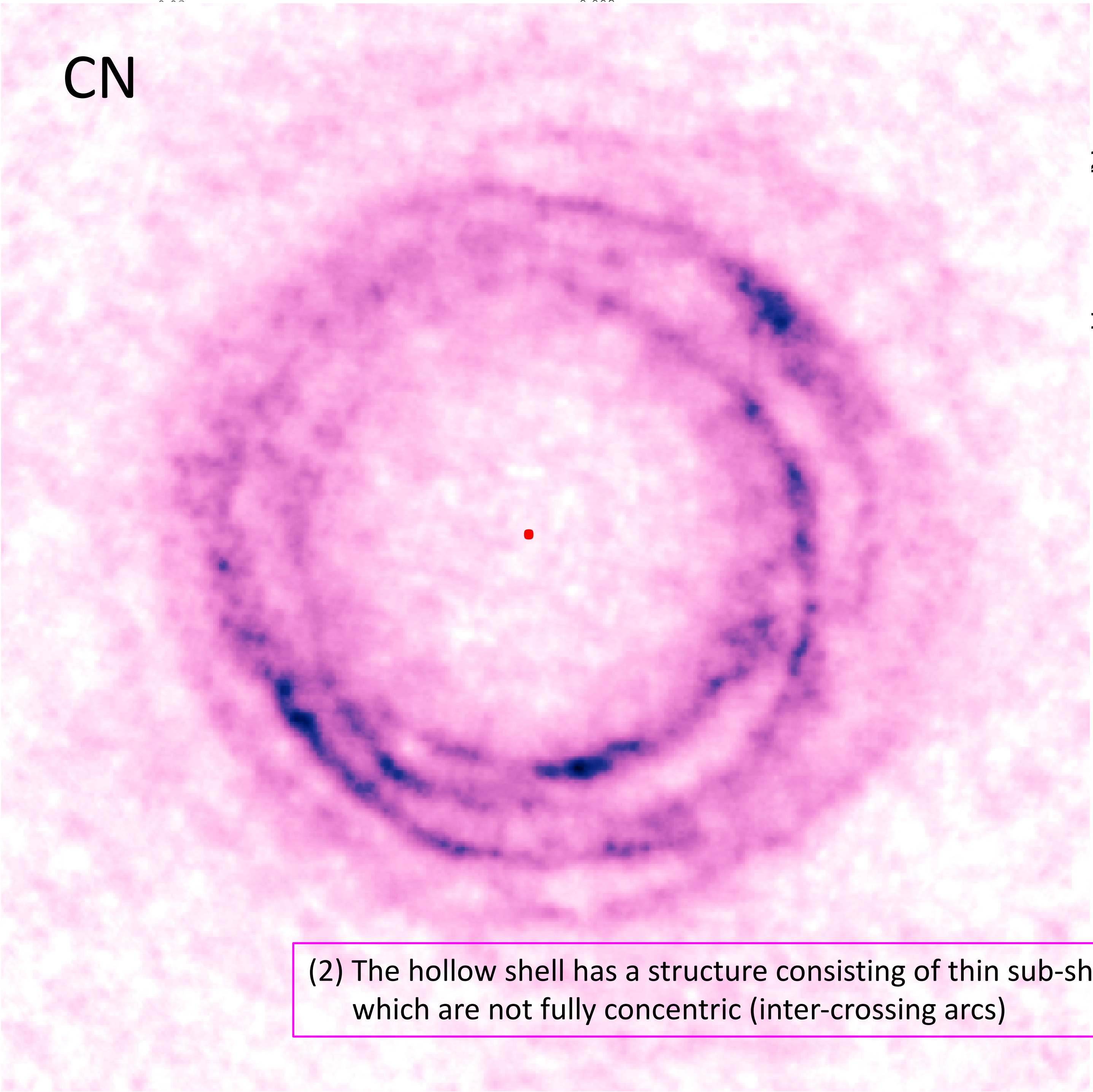

216

’)

cules

(2) The hollow shell has a structure consisting of thin sub-shells which are not fully concentric (inter-crossing arcs)

To get rid of the rich azimuthal structure and study only the radial behavior, we make an azimuth average of the brightness distributions

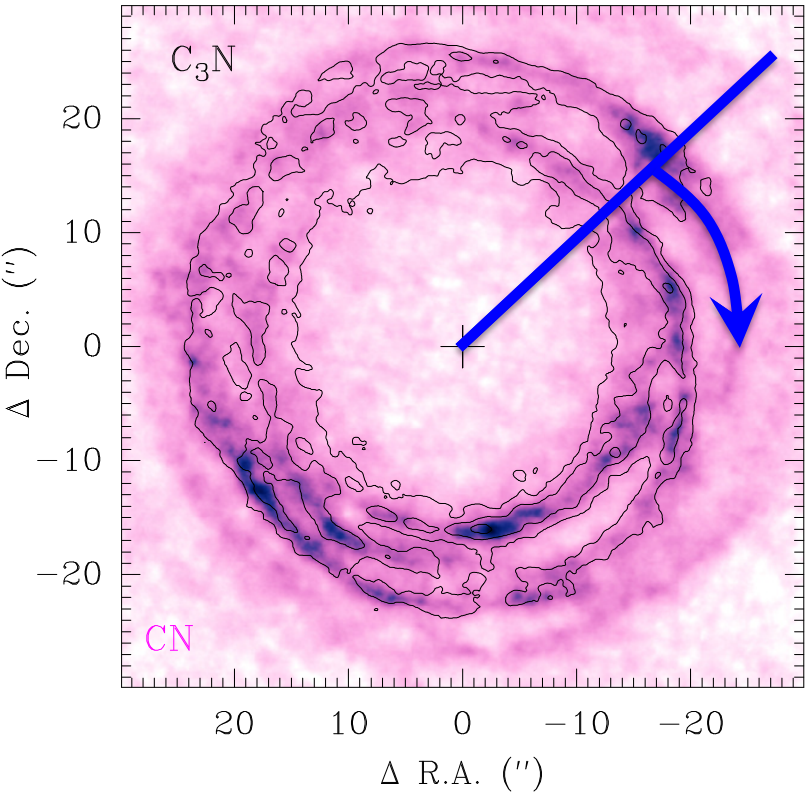

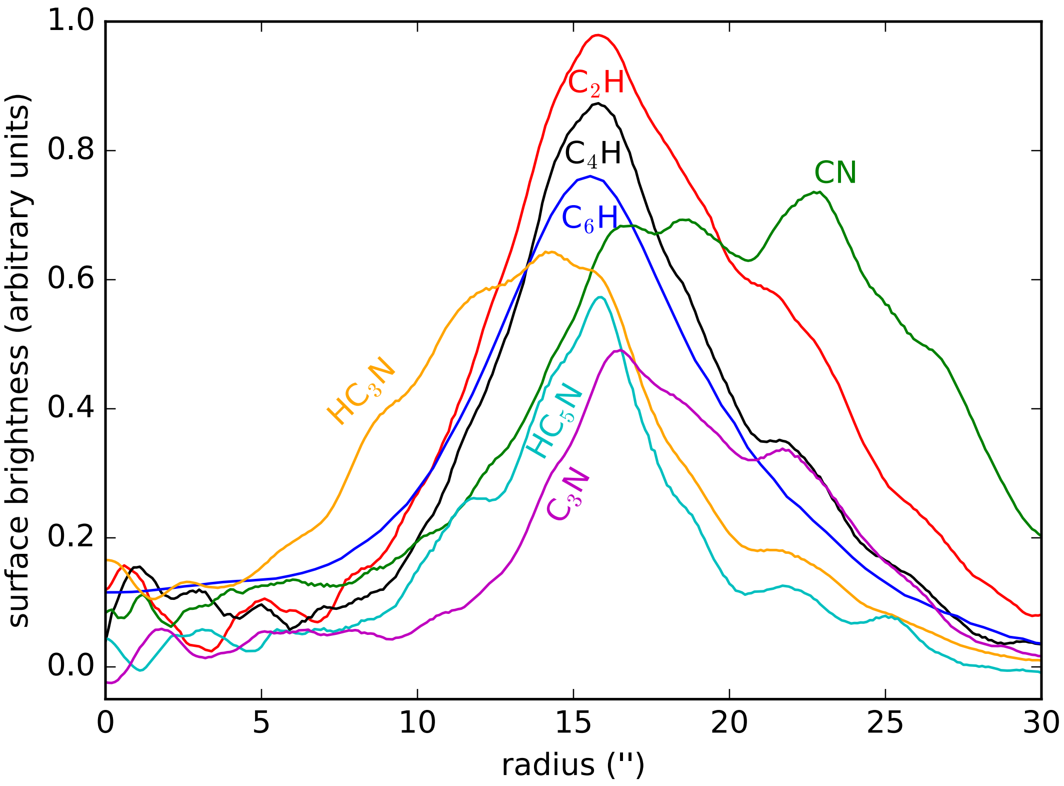

(7) Hydrocarbon radicals peak at the same radius
Cyanides show more disperse distributions: $HC_3N$ appears earlier and CN extends farther

# (Chemical + Excitation –collisional and **infrared** excitation-) Model vs Observations

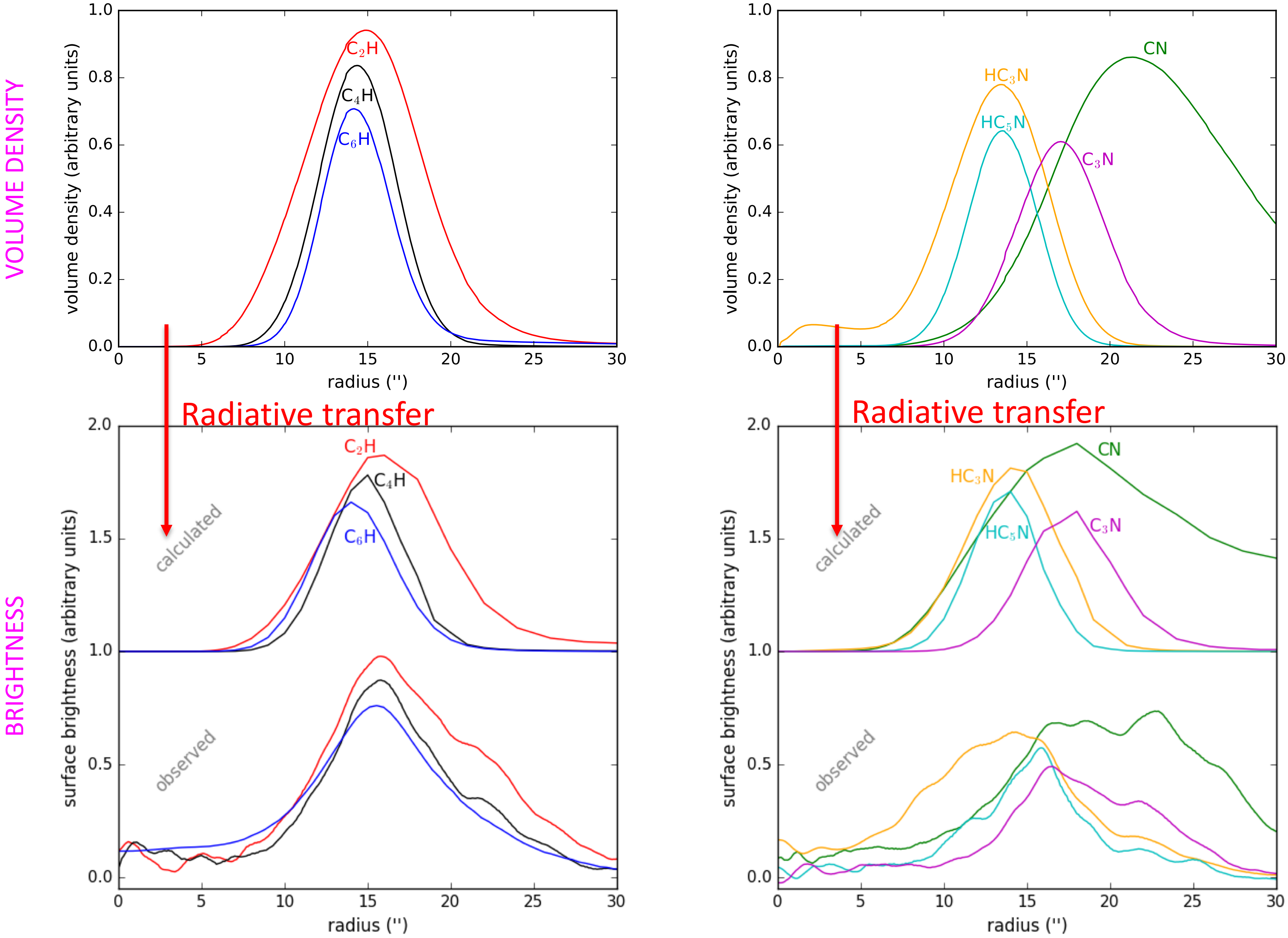

VOLUME DENSITY

BRIGHTNESS

Radiative transfer

Radiative transfer

Concluding remark:

The good agreement between model and observations validates this scenario of carbon chain growth In the external layers of the envelope (around 700 Stellar Radii)

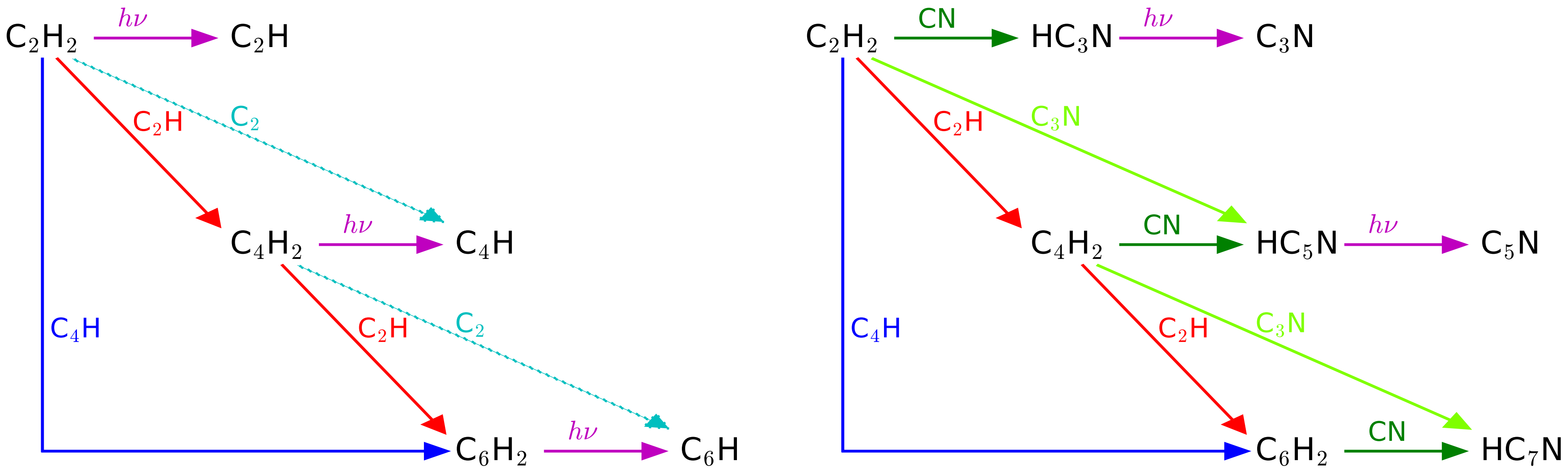

Polyyne growth is driven by reactions involving $C_2H$ and $C_4H$ radicals

CN produced in the photodissociation of HCN

Cyanopolyyne growth is driven by reactions involving CN and $C_3N$ radicals

The route $HC_3N \rightarrow HC_5N \rightarrow HC_7N \rightarrow$ … does not happen

Cyanopolyyne growth is intimately related to polyyne growth

The kinetics of most of these processes have been studied in the laboratory in recent years:

photodissociation cross section and low-temperature rate constants of chemical reactions.

**What about the $C_nH_2$ species ?** They lack of permanent dipole moment, hence, only detectable in the IR

# Conclusions : Astrophysical observations

- Carbon clusters detected in the external layers of the envelope
- $C_2$ and $C_3$ detected in the near and mid-IR in, and around, the photosphere
- $C_nH$ radicals up to $C_8H$ detected in the external layers of the envelope. Chemistry well understood (photochemistry)
- Cyanopolyynes and polyacetylenes are detected in the mid and external layers of the envelope (photochemistry)
- All carbon anions, $C_nH^-$, are formed in the external layers (electron attachment to the radicals $C_nH$)
- Dust is formed in the photosphere and growth in a region of 20 stellar radii
- The growth of Carbon clusters and dust seeds could occur in the photosphere, and around, but is probably kinetically limited by energetics and spin forbidden reactions.
- **LABORATORY SIMULATIONS NEEDED TO UNDERSTAND DUST FORMATION :: NANOCOSMOS**

# NANOCOSMOS

## *An ERC synergy project to understand how dust is formed*

CSIC

European Research Council
Established by the European Commission

NANOCOSMOS

# NANOCOSMOS A complementary and multidisciplinary team

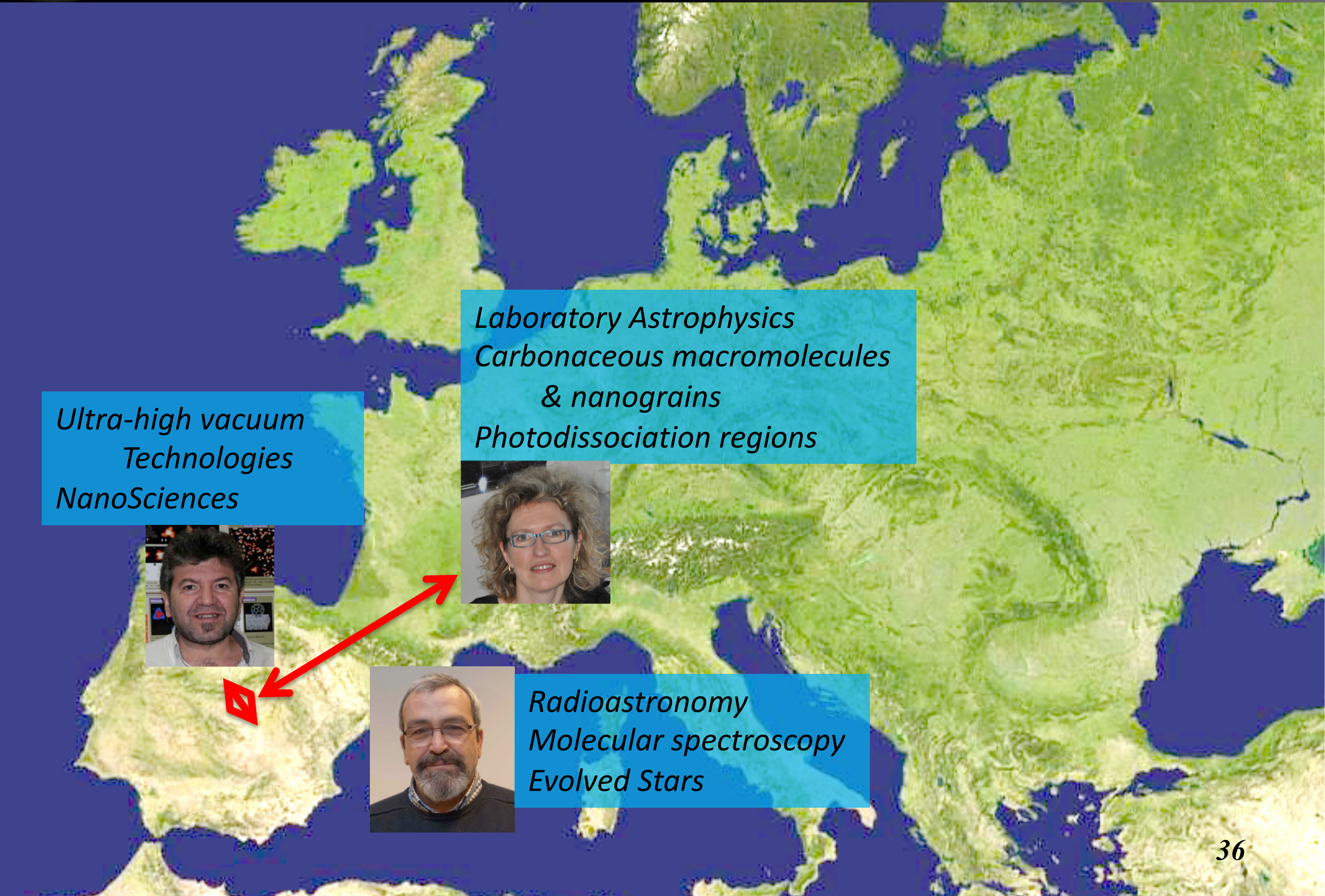

*Ultra-high vacuum*
*Technologies*
*NanoSciences*

*Laboratory Astrophysics*
*Carbonaceous macromolecules*
*& nanograins*
*Photodissociation regions*

*Radioastronomy*
*Molecular spectroscopy*
*Evolved Stars*

# *Beyond the current frontiers*

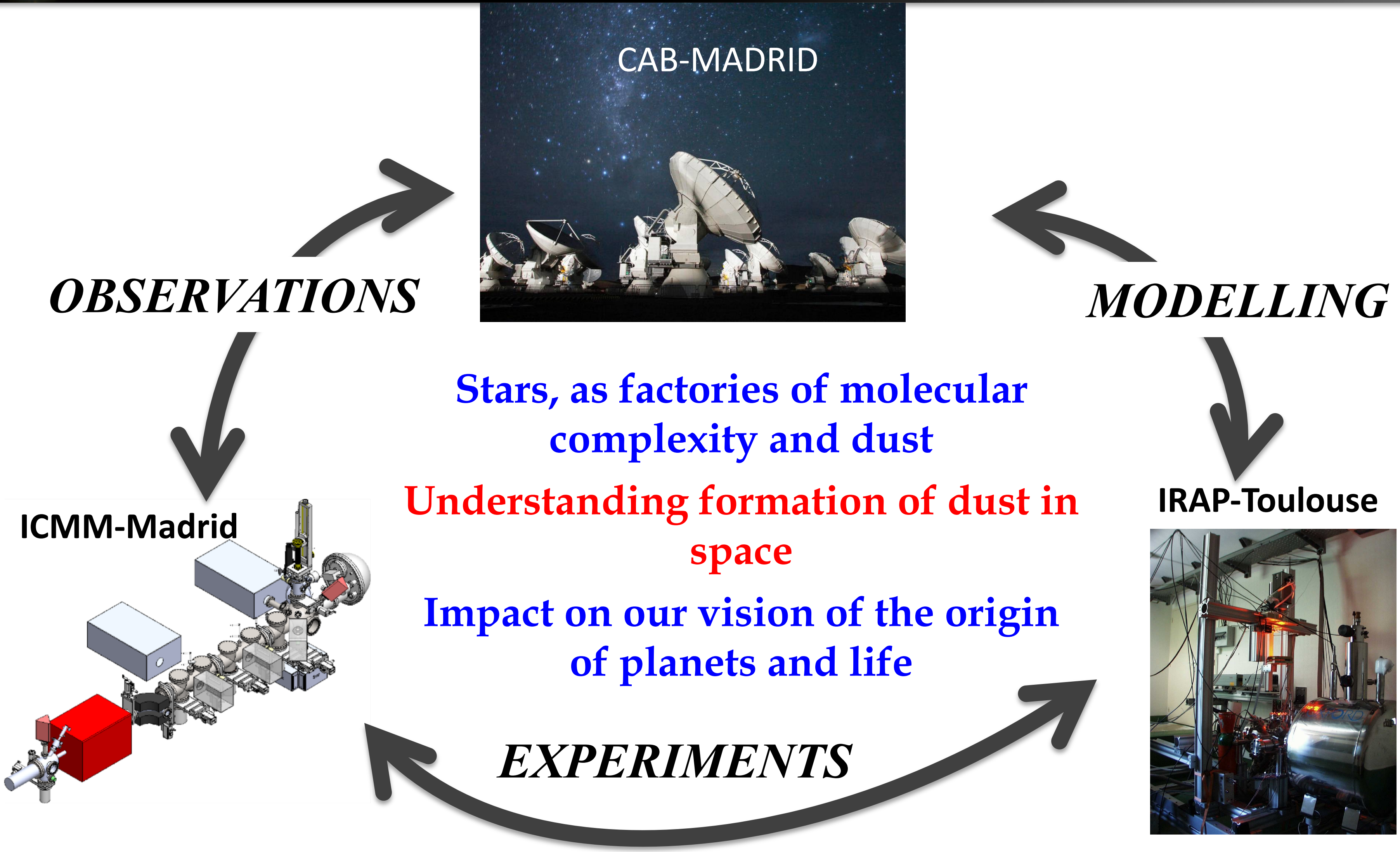

***OBSERVATIONS***

***MODELLING***

***EXPERIMENTS***

**Stars, as factories of molecular complexity and dust**

**Understanding formation of dust in space**

**Impact on our vision of the origin of planets and life**

***New scientific approaches through synergy***

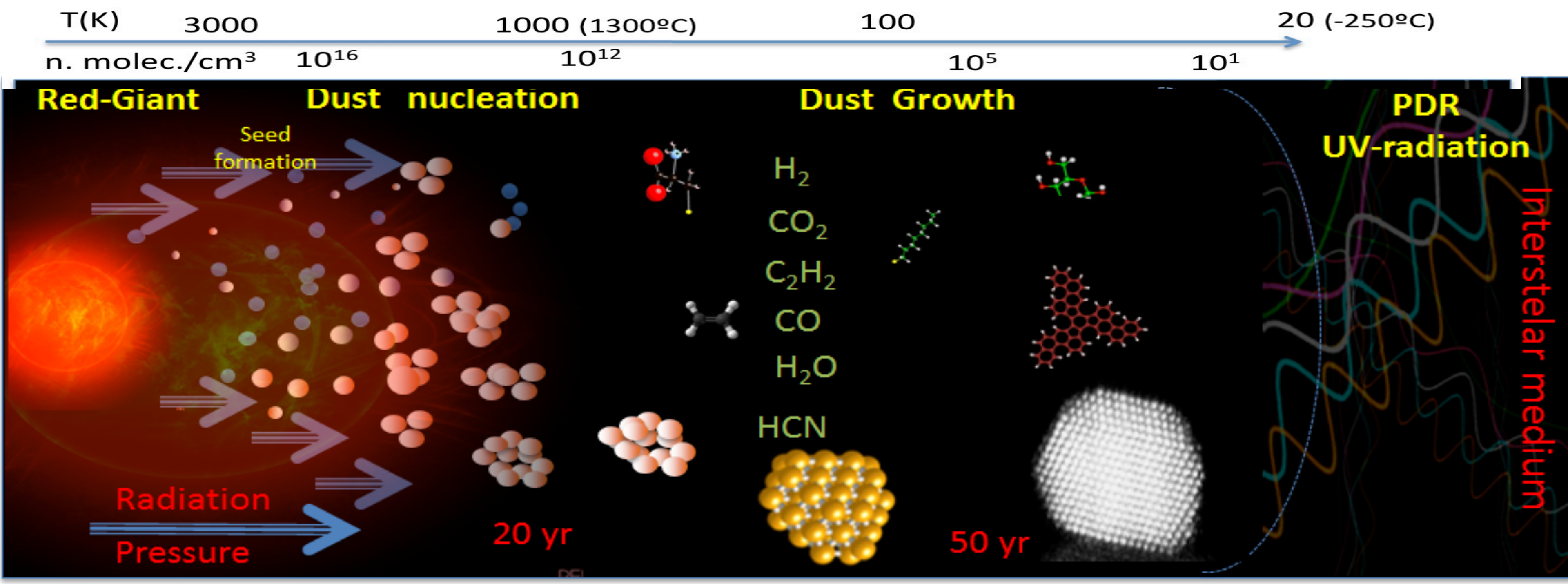

**Dust Nucleation**:
MICS + NEON

**Dust Growth**:
INTERACTION +
SPECTROSCOPY

**IEM and processing**
INFRA + ANA

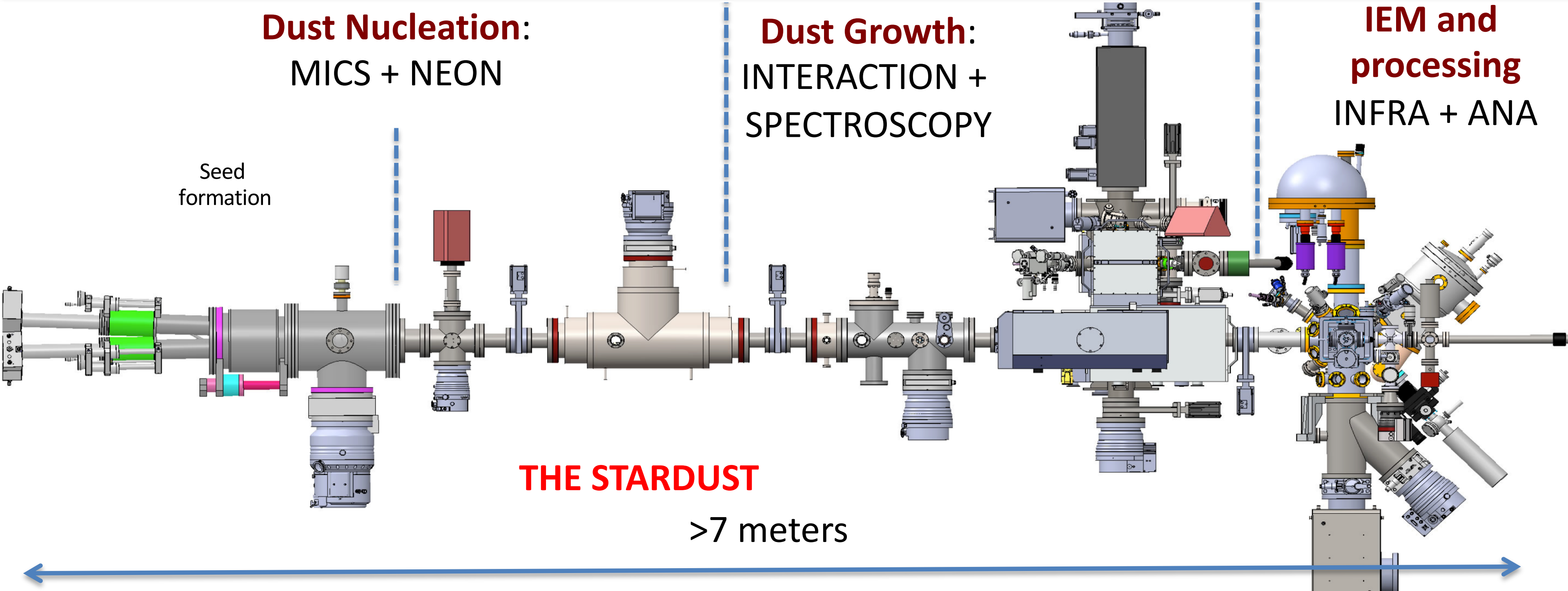

**THE STARDUST**

>7 meters

# The StarDust machine: current status September 2017

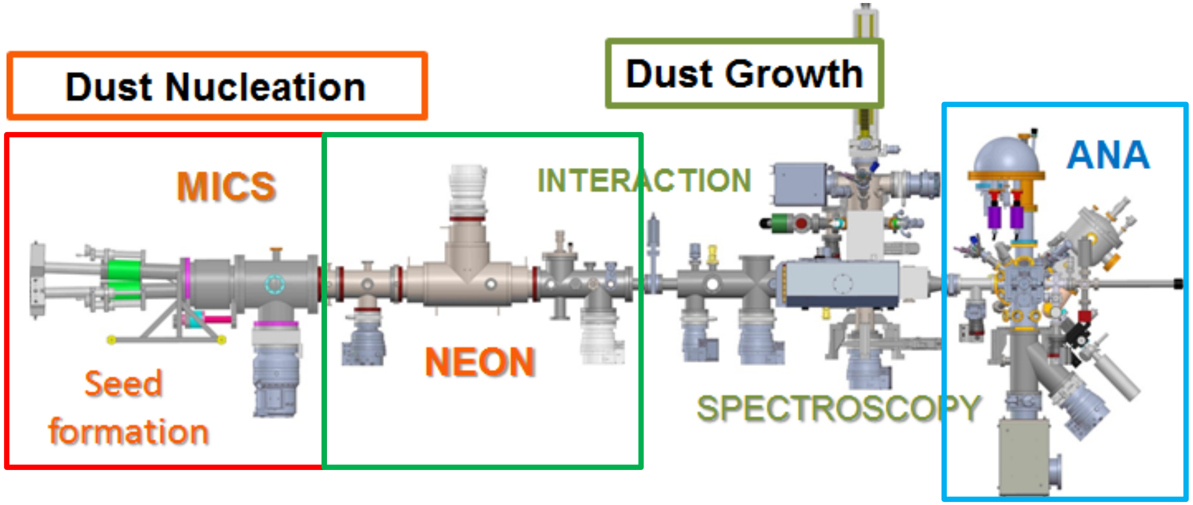

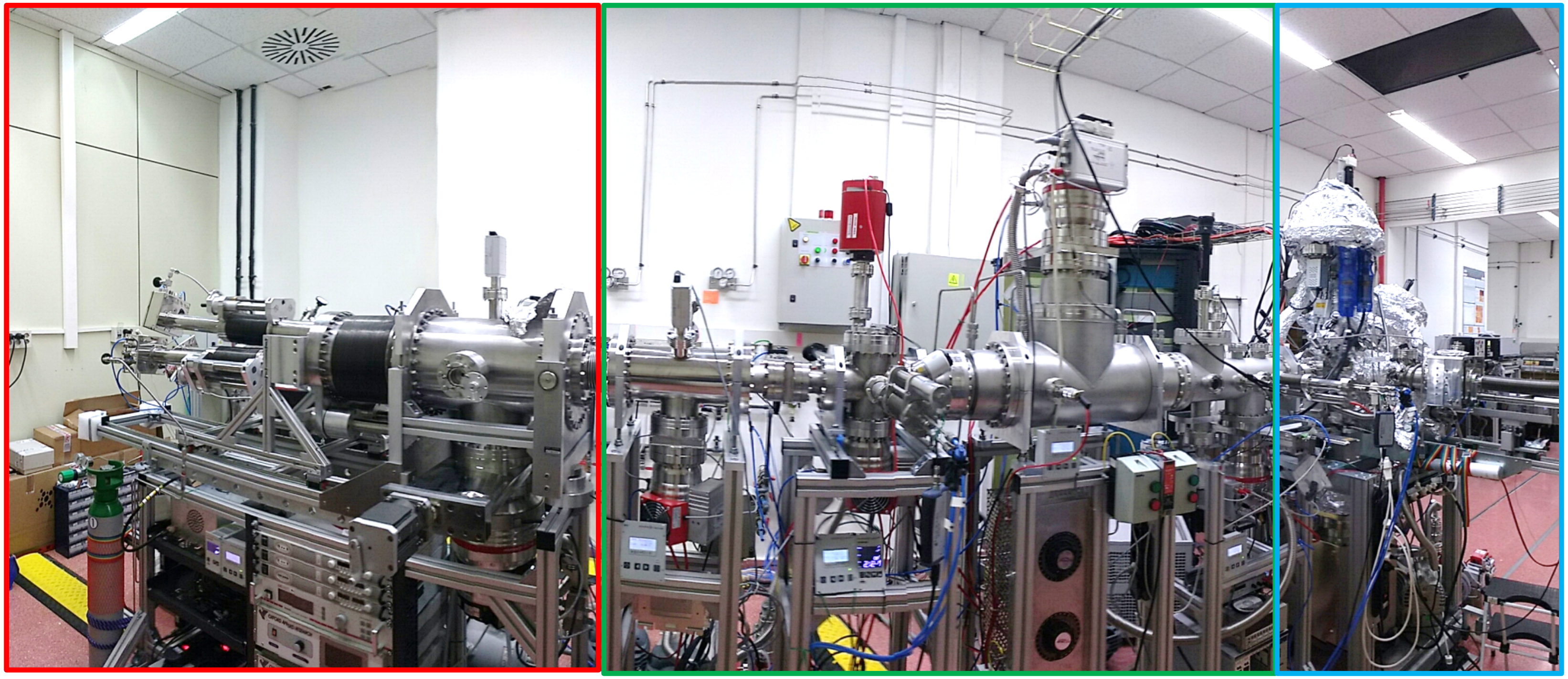

**ASTROPHYSICAL OBSERVATIONS AND NANOCOSMOS EXPERIMENTAL SETUPS**

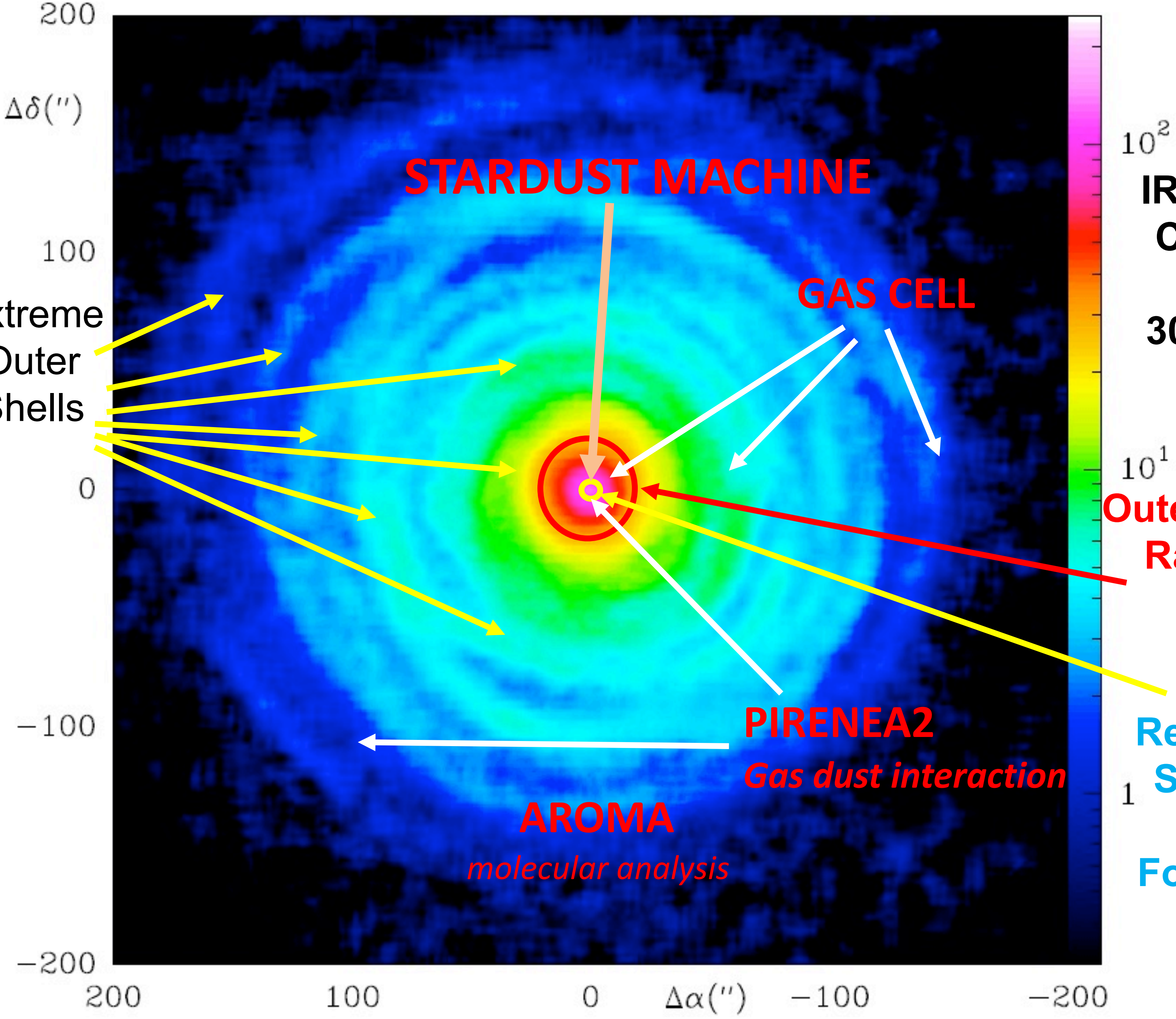

**STARDUST MACHINE**

**GAS CELL**

Extreme Outer Shells

**PIRENEA2**

*Gas dust interaction*

**AROMA**

*molecular analysis*

**IRC+10216**
**CO J=2-1**

**30m IRAM data**

**Outer carbon Radicals shell**

**Inner Refractory Species. Dust Formation Zone**

**ALMA**

# Sputtering of a **graphite** target with $Ar^+$ + **$H_2$ injection** in the aggregation zone

**$n(e^-) = n(Ar^+) \sim 10^{-4}\, n(Ar)$**

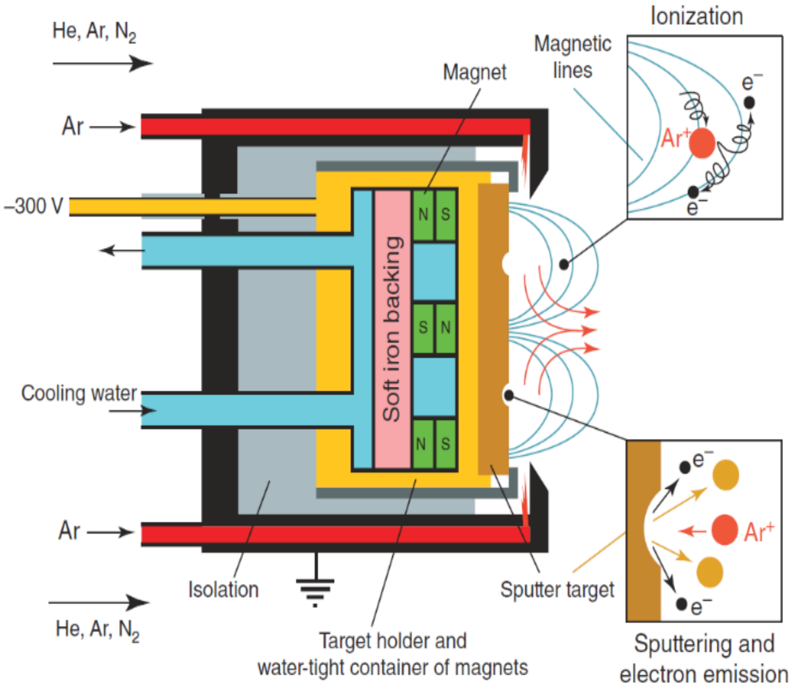

**Figure 1.4** The magnetron sputter head in more detail. A cylindrical magnetic field is used. Charge production and surface erosion are maximal in the region where the magnetic field is parallel to the surface, as indicated by the two inserts. Note that the argon gas is introduced in two different regions, (i) around the source and (ii) it is blown directly into the region where sputtering is maximal. The intensity and mass distribution of clusters can be optimized, by playing with these two gas flows. The sputter head has to be water-cooled.

*Gas-Phase Synthesis of Nanoparticles*. Edited by Yves Huttel (2017) Wiley-VCH.

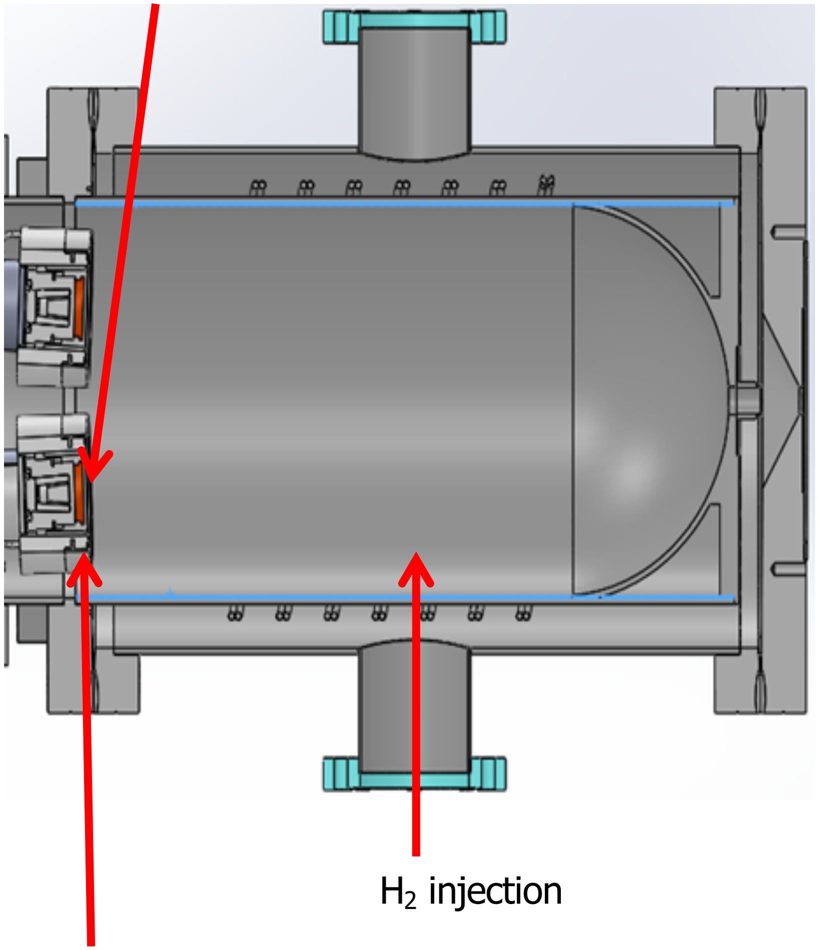

Graphite target

$H_2$ injection

Sputter gas (Ar) inlet

*No detection of any PAH in gas phase*

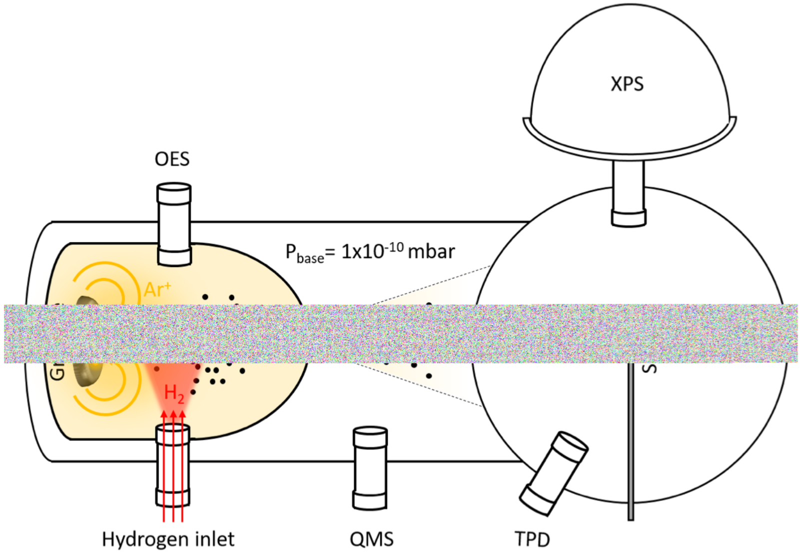

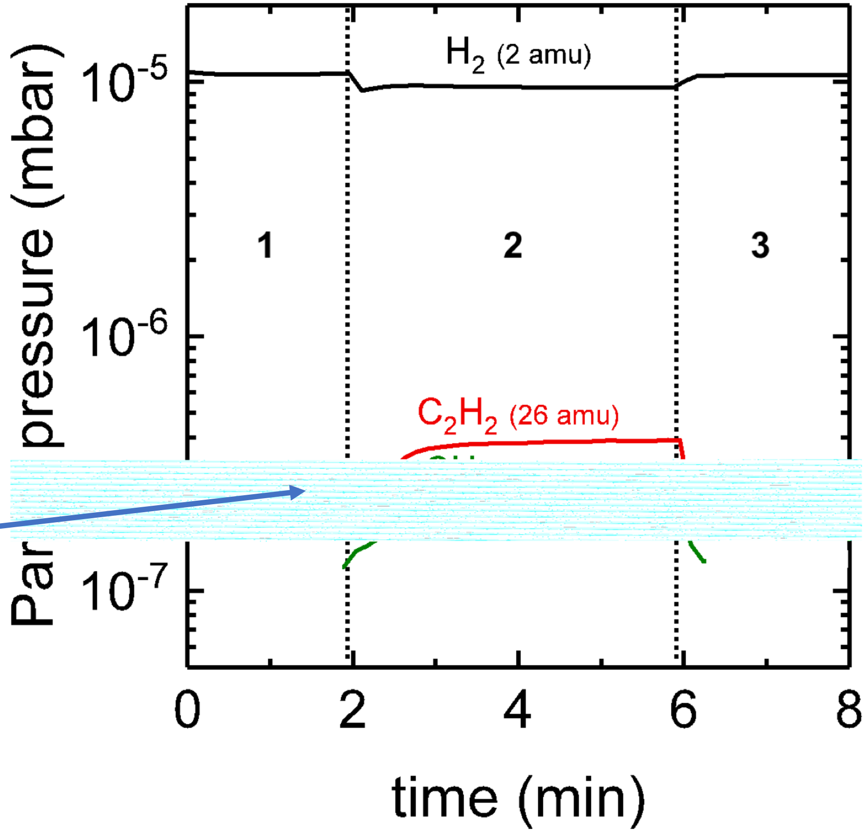

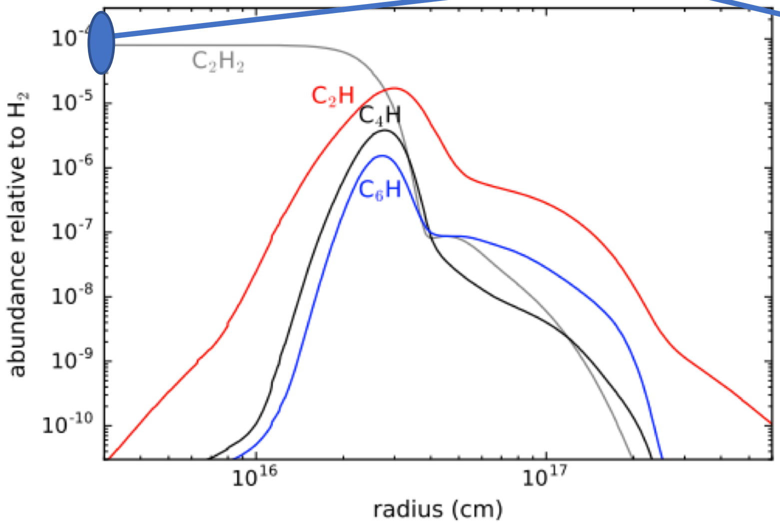

# $C_2$ and CH are rapidly consumed:  they are captured to form new species

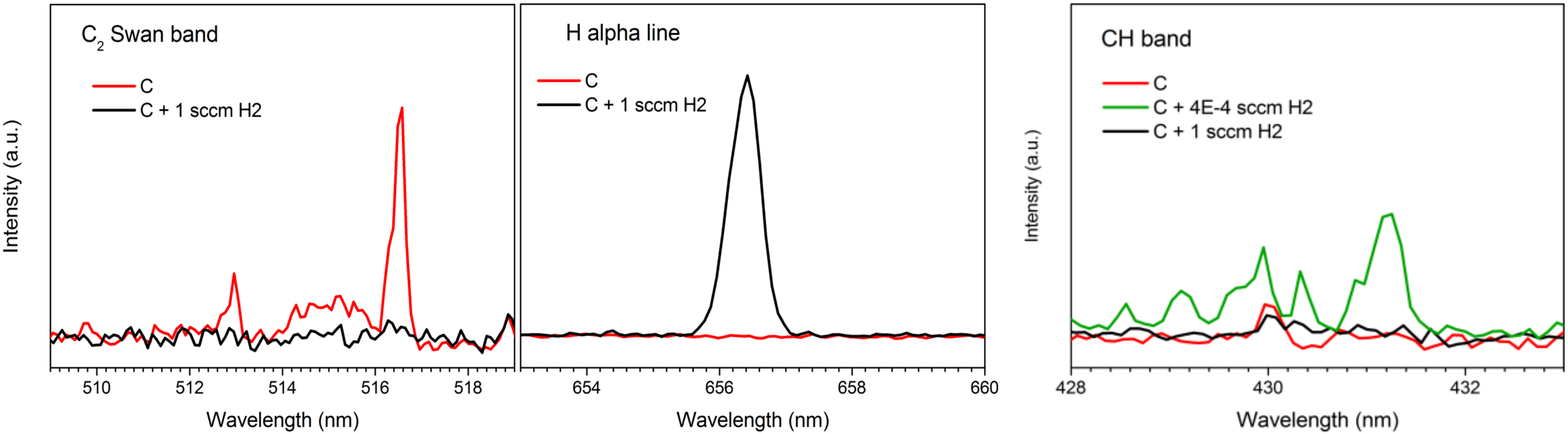

# XPS in-situ: The sp3 component grow up

No aromatic component

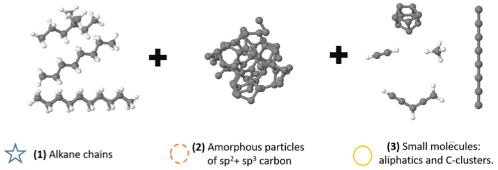

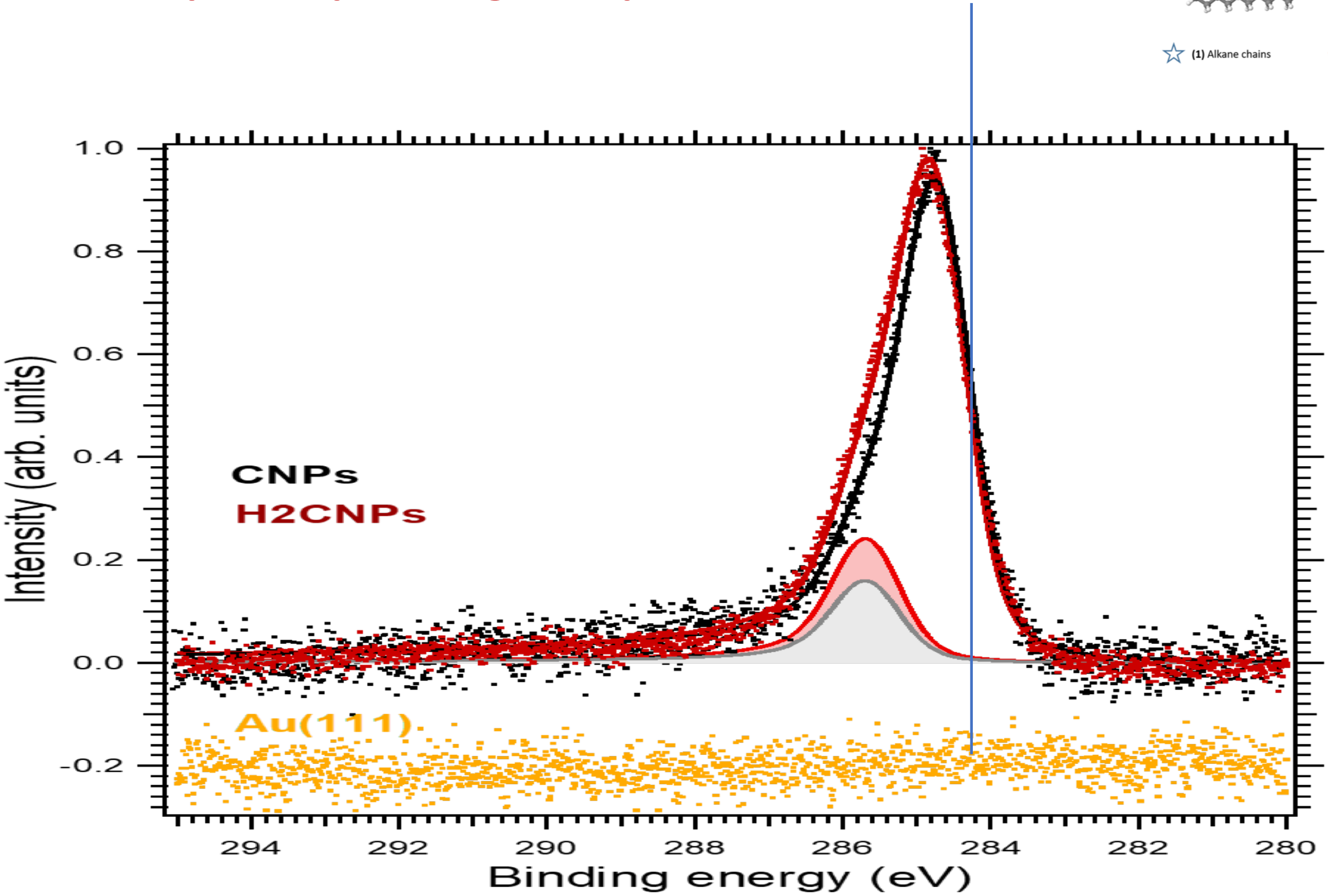

# A zoo of clusters and molecules

- Coverage 40%
- Different clases of atomic-scale adsorbates
  - Individual clusters
  - Self-organized Short chains
  - Self-organized Long chains
  - Ring-shaped clusters

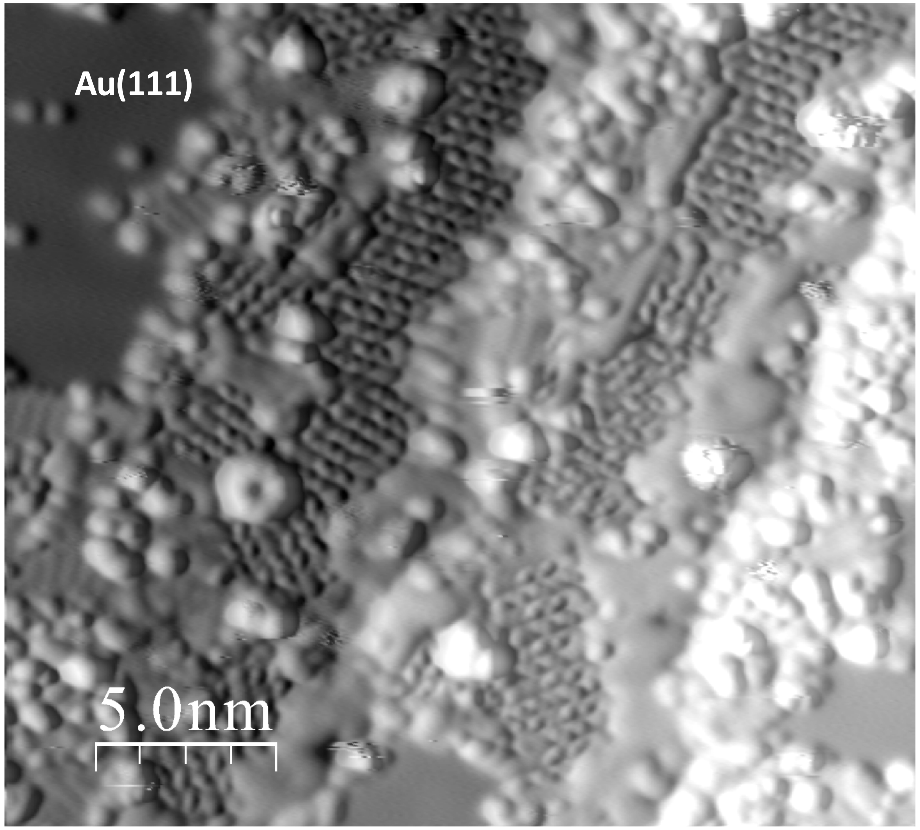

## Nano-sized amorphous grains

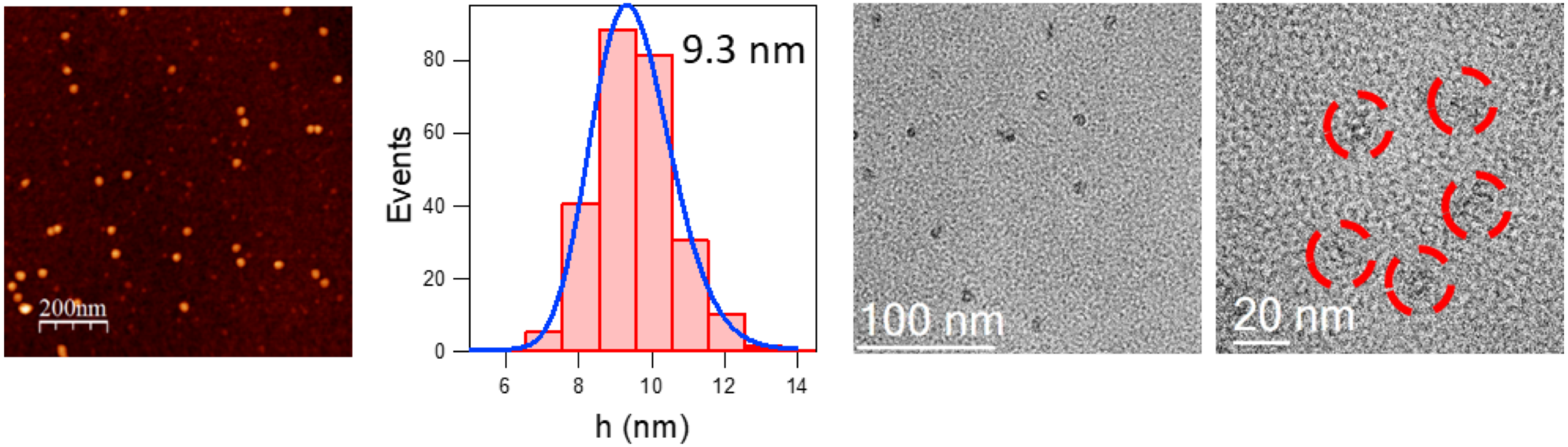

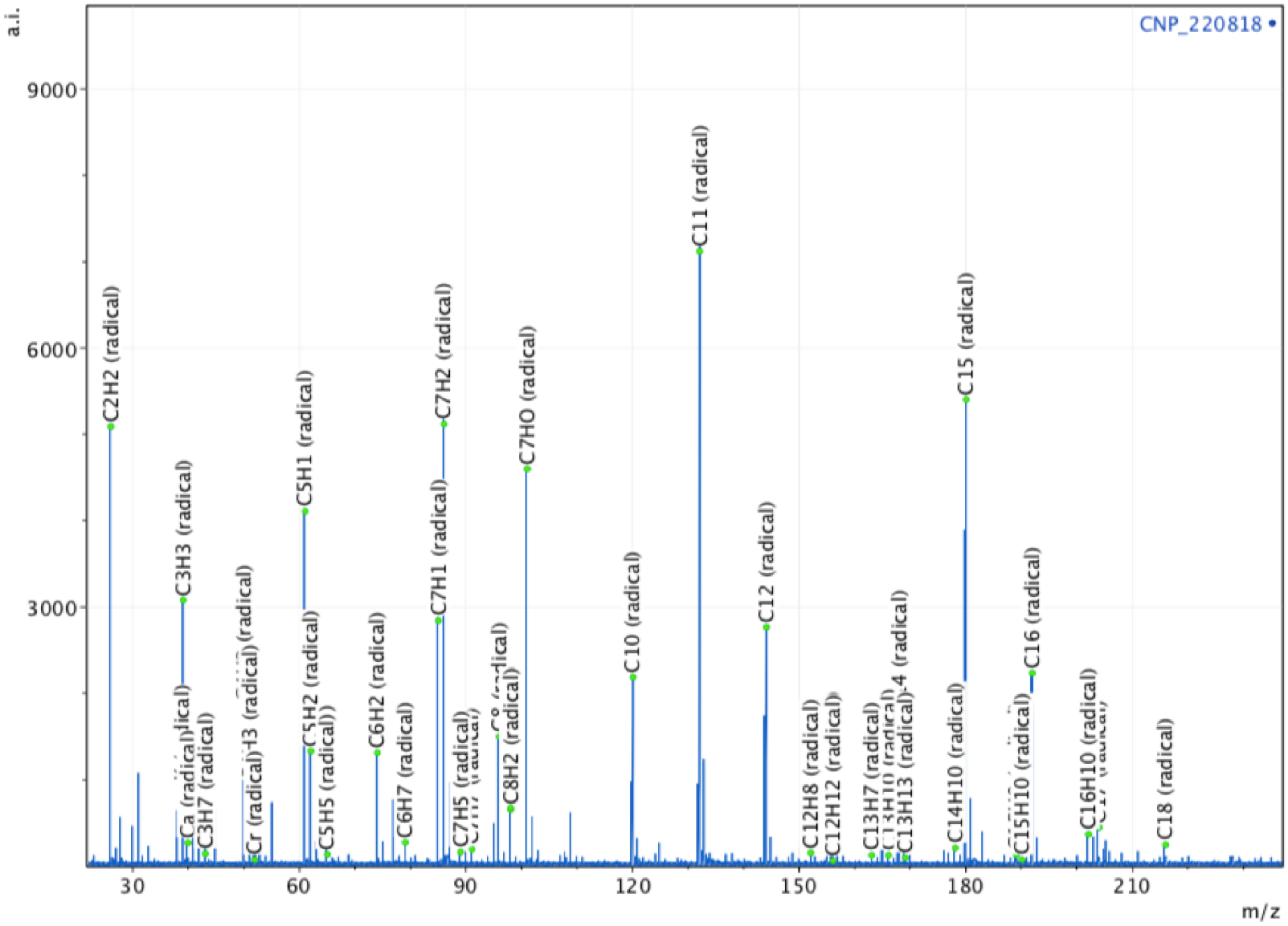
a.i.
CNP_220818
9000
6000
3000
30
60
90
120
150
180
210
m/z
C2H2 (radical)
C3H3 (radical)
Ca (radical)
C3H7 (radical)
Cr (radical)
C5H1 (radical)
C5H2 (radical)
C5H5 (radical)
C6H2 (radical)
C6H7 (radical)
C7H1 (radical)
C7H2 (radical)
C7H5 (radical)
C8H2 (radical)
C7HO (radical)
C10 (radical)
C11 (radical)
C12 (radical)
C12H8 (radical)
C12H12 (radical)
C13H7 (radical)
C13H13 (radical)
C14H10 (radical)
C15 (radical)
C15H10 (radical)
C16 (radical)
C16H10 (radical)
C18 (radical)

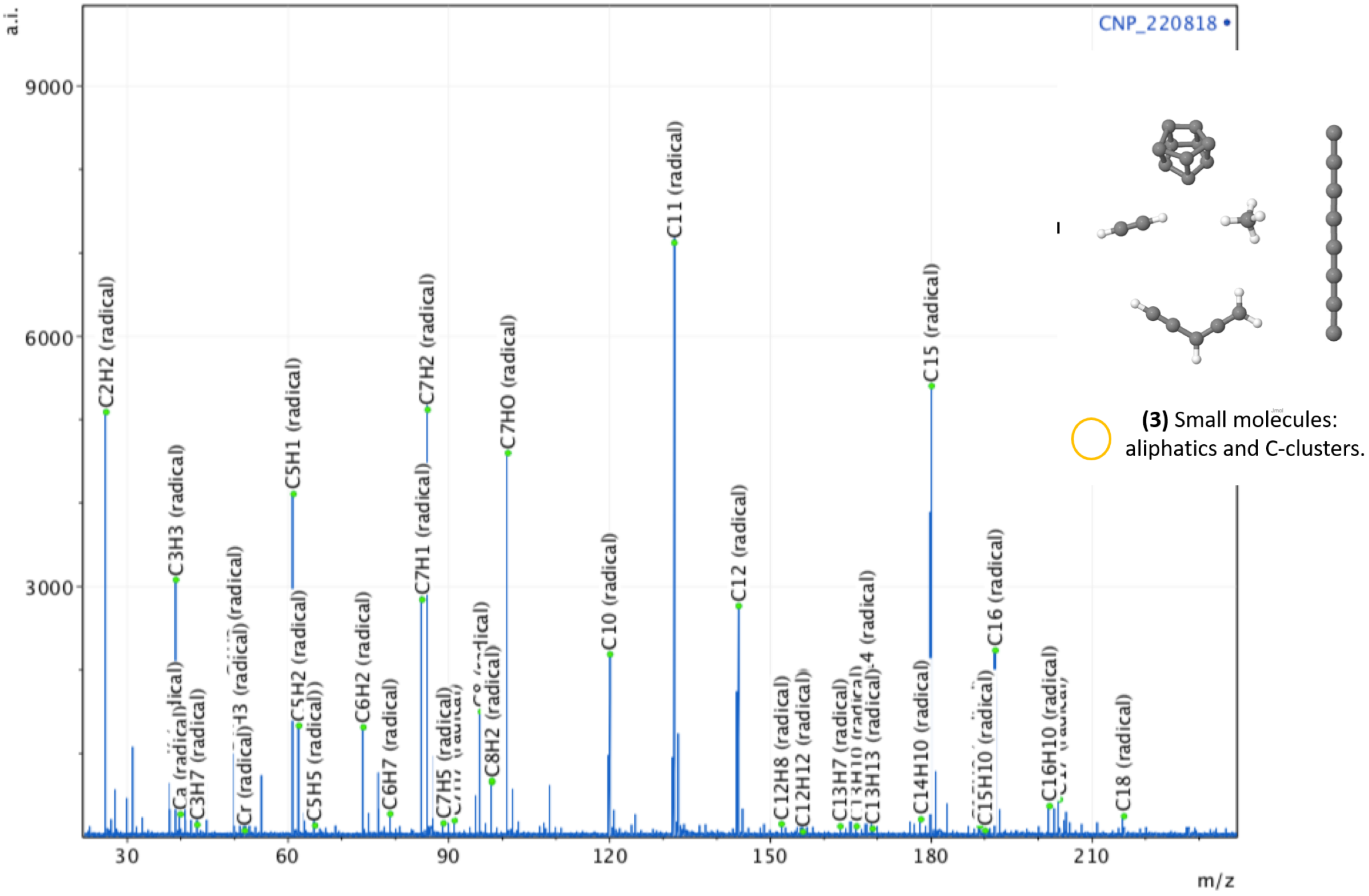

**(3)** Small molecules: aliphatics and C-clusters.

ARTICLE

Received 24 Jul 2013 | Accepted 3 Dec 2013 | Published 21 Jan 2014

DOI: 10.1038/ncomms4054

# Graphene etching on SiC grains as a path to interstellar polycyclic aromatic hydrocarbons formation

P. Merino[1], M. Švec[2], J.I. Martinez[3], P. Jelinek[2], P. Lacovig[4], M. Dalmiglio[4], S. Lizzit[4], P. Soukiassian[5,6], J. Cernicharo[1] & J.A. Martin-Gago[1,3]

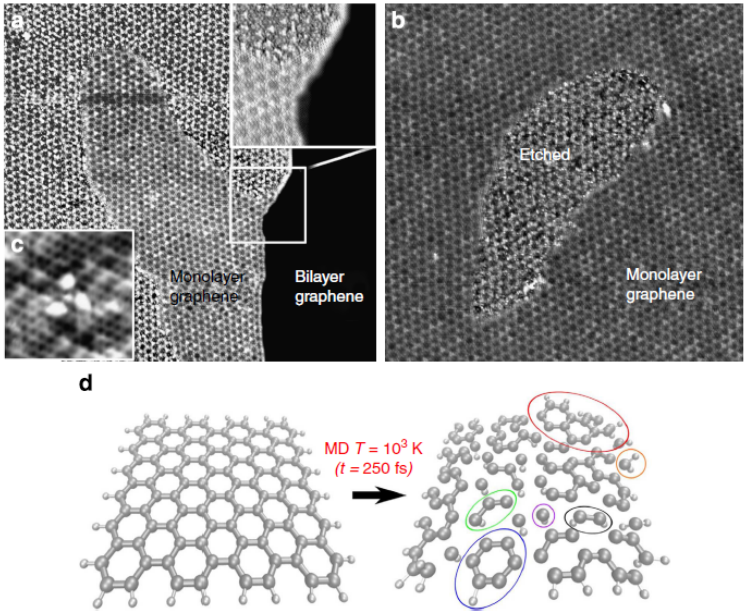

Polycyclic aromatic hydrocarbons as well as other organic molecules appear among the mo abundant observed species in interstellar space and are key molecules to understanding th prebiotic roots of life. However, their existence and abundance in space remain a puzzle. Here we present a new top-down route to form polycyclic aromatic hydrocarbons in large quantities in space. We show that aromatic species can be efficiently formed on the graphitized surface of the abundant silicon carbide stardust on exposure to atomic hydrogen under pressure and temperature conditions analogous to those of the interstellar medium. To this aim, we mimic the circumstellar environment using ultra-high vacuum chambers and investigate the SiC surface by *in situ* advanced characterization techniques combined with first-principles molecular dynamics calculations. These results suggest that top-down routes are crucial to astrochemistry to explain the abundance of organic species and to uncover the origin of unidentified infrared emission features from advanced observations.

Cite this: *Phys. Chem. Chem. Phys.*, 2016, **18**, 3489

# Laboratory astrochemistry: catalytic conversion of acetylene to polycyclic aromatic hydrocarbons over SiC grains

T. Q. Zhao,[a] Q. Li,[a] B. S. Liu,*[ab] R. K. E. Gover,[c] P. J. Sarre[c] and A. S.-C. Cheung*[a]

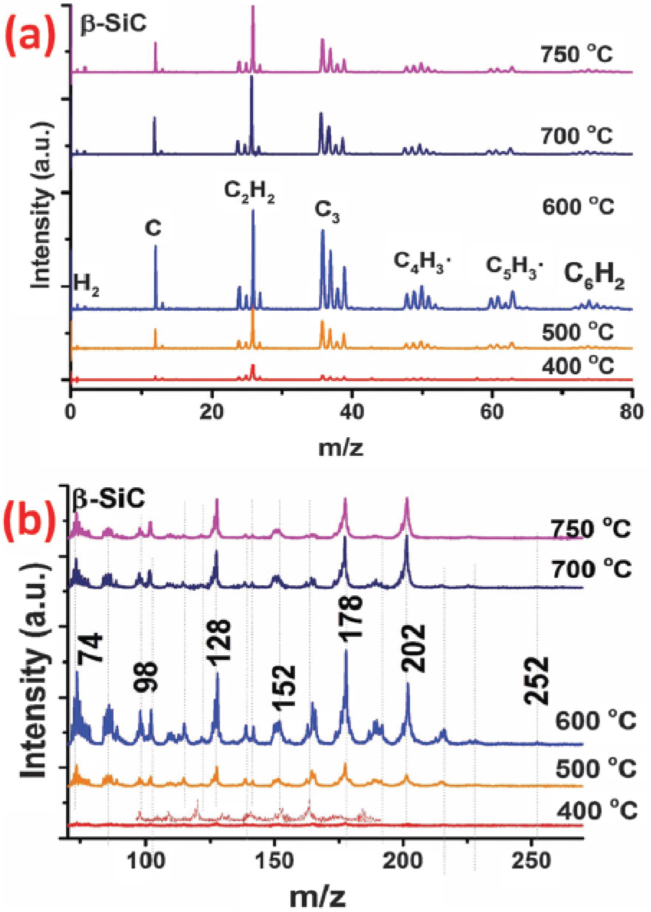

**Fig. 3** TOF-MS signals from acetylene conversion over β-SiC as a function of temperature in the mass range (a) 0–80 and (b) 75–275.

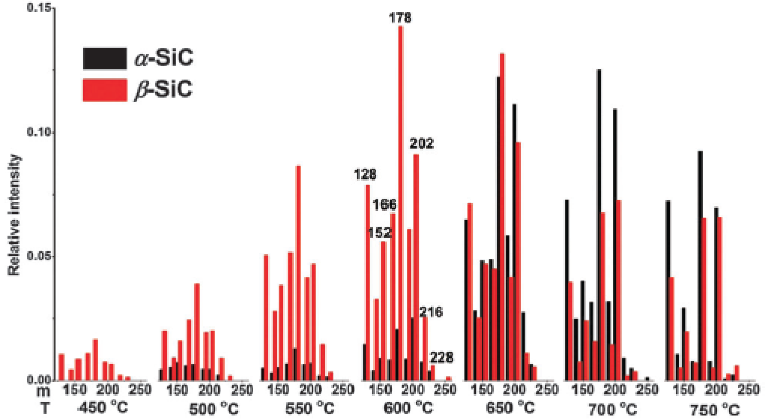

**Fig. 5** Comparison of PAH formation on β-SiC and α-SiC at different temperatures. The numerical values are the molecular weight of the PAHs formed.

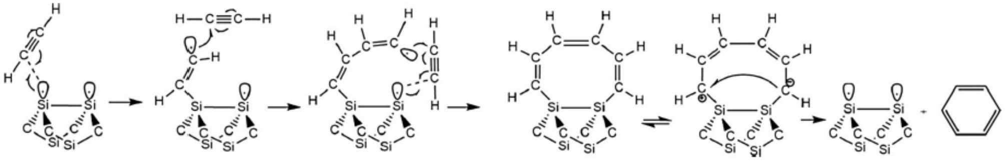

## *Astro-summary*

## Aliphatic nature of carbonaceous cosmic dust analogs produced mimicking dust nucleation zones

The MICS of the Stardust machine present conditions close to the dust formation zone of AGBs (density of C and $H_2$, and H)

Our experiments demonstrate that highly saturated hydrocarbons (alkane and aliphatic) can be efficiently formed in AGB stars and could condensate on grains. These alkane species are “invisible” in rotational spectroscopy. In IR spectroscopy they will be difficult to detect in astro objects  due to the large partition functions of these species.

So far only $C_2$, $C_3$, $C_4$, $C_5$, $C_2H_2$, $C_4H_2$, $C_2H_4$, $NH_3$ and $SiH_4$, have been detected in the infrared towards AGBs (IRC+10216). $C_2H_6$ searched but only upper limits have been obtained.

We have no found PAHs, just small traces. However, they could be formed through H and $C_2H_2$ reaction over SiC-dust surfaces (among many other possible paths).

$C_nH$ radicals can react with $H_2$ with very low barriers:   $C_nH + H_2 \Rightarrow C_nH_3$

# Acknowledgments: The STARDUST TEAM + NANOCOSMOS

erc SYNERGY nanoCOSMOS

José Cernicharo

Christine Joblin

CENTRO DE ASTROBIOLOGÍA
ASOCIADO AL NASA ASTROBIOLOGY INSTITUTE
CSIC INTA

ICTP
Instituto de Ciencia y Tecnología de Polímeros

IEM INSTITUTO DE ESTRUCTURA DE LA MATERIA